

A NEW CRANIUM OF *CROCODYLUS ANTHROPOPHAGUS* FROM OLDUVAI GORGE, NORTHERN TANZANIA

BEATRICE AZZARÀ¹, GIOVANNI BOSCHIAN^{2,3}, CHRISTOPHER A. BROCHU⁴,
MASSIMO DELFINO^{5,6}, DAWID A. IURINO^{1,7}, JACKSON S. KIMAMBO⁸, GIORGIO MANZI⁹,
FIDELIS T. MASAO¹⁰, SOFIA MENCONERO¹¹, JACKSON K. NJAU^{12,13} & MARCO CHERIN^{1*}

¹Dipartimento di Fisica e Geologia, Università degli Studi di Perugia, Via Alessandro Pascoli, 06135 Perugia, Italy.

E-mail: beatrice.azzara@studenti.unipg.it, marco.cherin@unipg.it

²Dipartimento di Biologia, Università di Pisa, Via Derna, 56126 Pisa, Italy. E-mail: giovanni.boschian@unipi.it

³Palaeo-Research Institute, University of Johannesburg, P.O. Box 524, Auckland Park, 2006, South Africa.

⁴Department of Earth & Environmental Sciences, University of Iowa, Iowa City, IA 52242, USA. E-mail: chris-brochu@uiowa.edu

⁵Dipartimento di Scienze della Terra, Università degli Studi di Torino, Via Valperga Caluso 35, 10125 Torino, Italy.

E-mail: massimo.delfino@unito.it

⁶Institut Català de Paleontologia Miquel Crusafont, Universitat Autònoma de Barcelona, Edifici ICTA-ICP, c/ Columnes s/n, Campus de la UAB, 08193 Cerdanyola del Vallès, Barcelona, Spain.

⁷PaleoFactory, Dipartimento di Scienze della Terra, Sapienza Università di Roma, Piazzale Aldo Moro 5, 00185 Roma, Italy.

E-mail: dawid.iurino@uniroma1.it

⁸Evolutionary Studies Institute, University of Witwatersrand, Private Bag 3, Wits 2050 Johannesburg, South Africa.

E-mail: kimambojackson@gmail.com

⁹Dipartimento di Biologia Ambientale, Sapienza Università di Roma, Piazzale Aldo Moro 5, 00185 Roma, Italy.

E-mail: giorgio.manzi@uniroma1.it

¹⁰Department of Archaeology & Heritage, College of Humanities, University of Dar es Salaam, P.O. Box 35050, Dar es Salaam, Tanzania.

E-mail: fitman@udsm.ac.tz

¹¹Dipartimento di Storia, Disegno e Restauro dell'Architettura, Sapienza Università di Roma, Piazza Borghese 9, 00186 Roma, Italy.

E-mail: sofia.menconero@uniroma1.it

¹²Department of Earth and Atmospheric Sciences, Indiana University, 1001 East 10th Street, IN 47405-1405 Bloomington, USA.

E-mail: jknjau@indiana.edu

¹³The Stone Age Institute, 1392 W. Dittmore Road, IN 47407-5097, Bloomington, USA.

*Corresponding author

To cite this article: Azzarà B., Boschian G., Brochu C.A., Delfino M., Dawid A., Iurino D.A., Kimambo J.S., Manzi G., Masao F.T., Menconero S., Njau J.K. & Cherin M. (2021) - A new cranium of *Crocodylus anthropophagus* from Olduvai Gorge, northern Tanzania. *Riv. It. Paleontol. Strat.*, 127(2): 275-295.

Keywords: Africa; crocodile; Crocodylidae; Early Pleistocene; Olduvai.

Abstract. Olduvai Gorge (northern Tanzania) is one of the best known and most iconic palaeontological and archaeological sites in the world. In more than a century of research it has yielded an impressive record of fossils and stone tools which stands as a compendium of human evolution in the context of environmental changes of East Africa in the last 2 Ma. Recent field work in the DK site at Olduvai lead to the retrieval of a partial crocodile cranium nicknamed Black Sun because it was discovered during an annular solar eclipse. The specimen is here described and compared with extinct and extant African crocodylids. The new cranium can be referred to *Crocodylus anthropophagus*, a Pleistocene species hitherto found only in Olduvai Gorge. Thanks to the good preservation of the skull table, its morphology is here characterised for the first time. Black Sun represents to date the earliest (ca. 1.9–1.85 Ma) and the most informative cranium of *C. anthropophagus* in the fossil record. Our phylogenetic analysis supports a strict relationship between *C. anthropophagus* and *Crocodylus thorbjarnarsoni*, a large species from the Plio-Pleistocene of the Turkana Basin (Kenya). These two sister taxa share a combination of characters which places them at the base of *Crocodylus*, providing an intriguing element to the debate on the African or extra-African origin of this genus.

Received: January 26, 2021; accepted: May 05, 2021

INTRODUCTION

Crocodylus is the most widely distributed crocodylian genus. It includes 13 recognized extant species occurring in the intertropical belt in Australia, South Asia, Africa, and America (Trutnau & Sommerlad 2006; Uetz et al. 2020). It also includes the largest living reptiles.

Phylogenetic analyses based on molecular and morphological data concur in indicating that the two species of *Crocodylus* currently recognized in Africa, *C. niloticus* and *C. suchus* (Neoafrikan *Crocodylus sensu* Cossette et al. 2020), are closely related to extant Neotropical crocodiles: *Crocodylus intermedius*, *Crocodylus moreletii*, *Crocodylus acutus*, and *Crocodylus rhombifer* (e.g., Brochu 2000, 2007; Oaks 2011; Meredith et al. 2011; Delfino et al. 2020; Pan et al. 2020). The late Miocene (ca. 7 Ma) African *Crocodylus checcchiai* may offer a biogeographic and phylogenetic link between the African and American clades based on a recent reassessment of material from Libya (Delfino et al. 2020), though other analyses suggest a more basal position for the species or its close relative in Kenya (Brochu & Storrs 2012).

In addition to Neoafrikan *Crocodylus*, two other crocodylid lineages are recognized in Africa (McAliley et al. 2006; Trutnau & Sommerlad 2006; Eaton et al. 2009; Hekkala et al. 2010; Meredith et al. 2011; Shirley et al. 2014, 2018; Smolensky 2015). The two species of slender-snouted crocodile (*Mecistops*) and three species of dwarf crocodile (*Osteolaemus*) are confined to wetlands of West and Central Africa, whereas the Neoafrikan *Crocodylus* has an extensive distribution throughout the continent and Madagascar (Isberg et al. 2019). Although species within these two complexes can be distinguished on subtle morphological grounds (Brochu 2007; Eaton et al. 2009; Shirley et al. 2014, 2018), significant consistent skeletal differences have not yet been identified that distinguish the two species of Neoafrikan *Crocodylus*.

Historically, the name *Crocodylus* has been used for any crocodylian fossil that shared some similarities to modern crocodiles, which over the time has been stereotyped as an ancient group of morphologically conservative “living fossils” that originated during the late Cretaceous (Lydekker 1886; Mook 1927; Mook & Brook 1933; Kálin 1955; Sill 1968; Steel 1973; Markwick 1998). In contrast, time-calibrated molecular analyses typically put the last

common ancestor of extant *Crocodylus* in the middle to late Miocene between 8 and 15 Ma (e.g., Oaks 2011; Pan et al. 2020). At least some biogeographic models place this origin in Asia (Nicolai & Matzke 2019), from where *Crocodylus* dispersed to Africa and Mediterranean Europe towards the New World (Brochu 2001; Oaks 2011; Meredith et al. 2011; Delfino et al. 2020). *Crocodylus palaeindicus* from the middle Miocene-Pleistocene of the Indian subcontinent (Siwalik sequence) and neighbouring areas may represent the earliest representative of the genus (Brochu 2000; Iijima et al. 2021). In addition to those of *C. palaeindicus*, other early remains referred (in some cases tentatively) to this genus are found in Africa (e.g., Johanson et al. 1982; Schrenk et al. 1995; Brochu & Storrs 2012; Brochu 2020; Delfino et al. 2020) and Southern Europe (Delfino et al. 2007; Delfino & Rook 2008; Delfino & Rossi 2013; Delfino et al. 2021), all in strata of similar age (late Miocene-Pliocene). Most likely, the circumtropical radiation of *Crocodylus* occurred during a period of increased extinction of other crocodylomorphs, which has been attributed to global cooling and aridification (Markwick 1998; Oaks 2011; Bronzatti et al. 2015; Mannion et al. 2015; De Celis et al. 2020; Solórzano et al. 2020). This major extinction phase started in the late Miocene, culminated in the Pliocene, and resulted in major declines in diversity of South American, African, and European crocodylians (Scheyer et al. 2013; Mannion et al. 2015; Moreno-Bernal et al. 2016; Cossette et al. 2020).

The African fossil record of *Crocodylus* is rich, though species-level referrals are not always robust. Although *Crocodylus niloticus* has been reported in the area from as far back as the late Miocene (e.g., Storrs 2003), occurrences earlier than the Pleistocene are generally viewed skeptically (Delfino et al. 2004; Brochu & Storrs 2012). Maccagno (1947) established *C. checcchiai* based on exceptionally preserved crania from the latest Miocene of Libya, one of which has been recently re-described by Delfino et al. (2020). Additional material possibly referable to the same species was reported from the late Miocene of Kenya (Brochu & Storrs 2012). The latter authors also established the giant-sized species *Crocodylus thorbjarnarsoni* from the Plio-Pleistocene of the Lake Turkana Basin (Kenya). Finally, the horned crocodile *Crocodylus anthropophagus* was described by Brochu et al. (2010) based on Early Pleistocene cranial and postcranial material from Olduvai Gorge

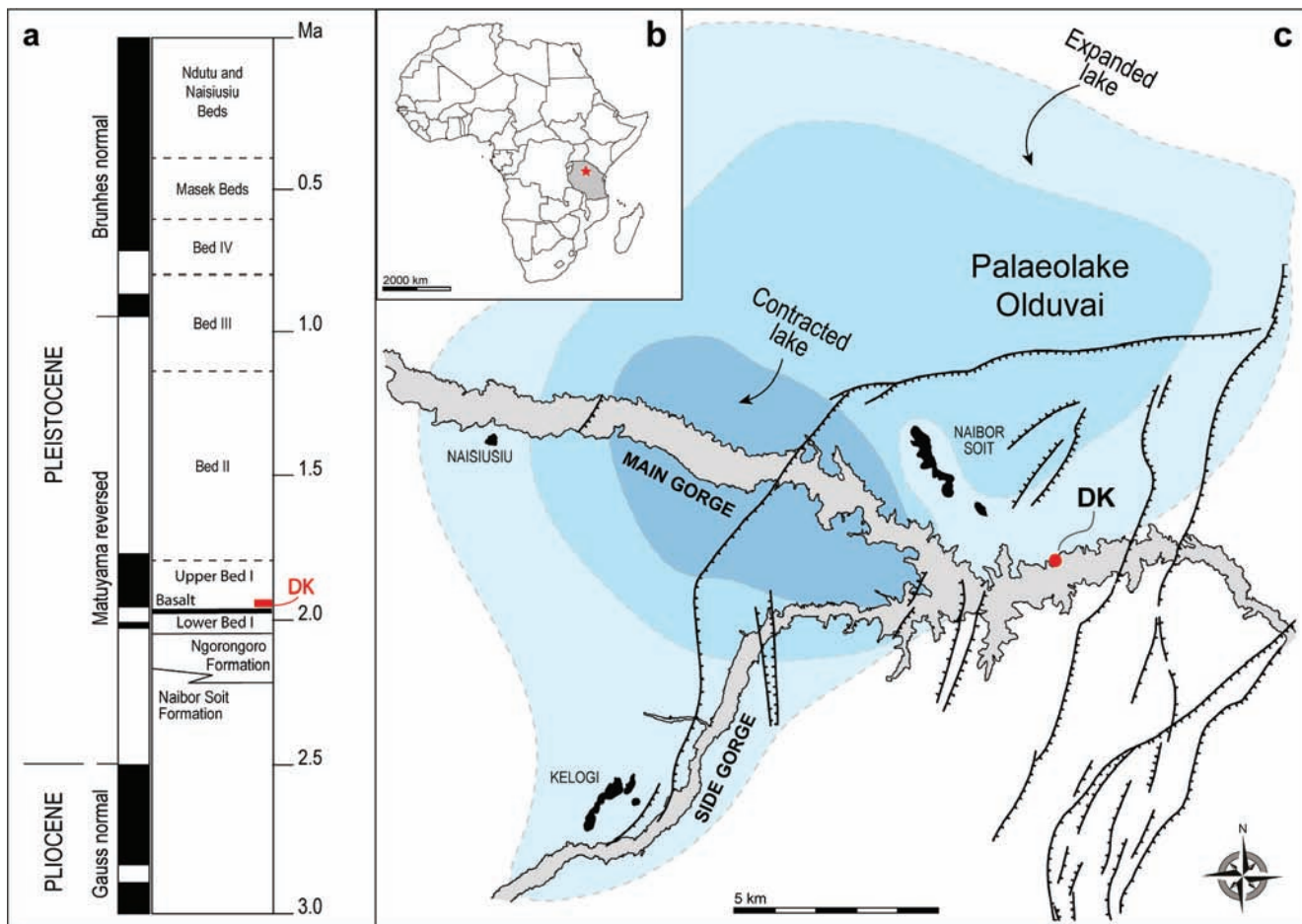


Fig. 1 - Stratigraphy and location of Olduvai Gorge. a) Stratigraphy (modified from Hay 1976 and Stanistreet et al. 2020a). The stratigraphic position of the DK sequence is shown in red. b) Location of Olduvai Gorge in northern Tanzania. c) Outline map (modified from Jorajev et al. 2016) with location of DK site. The reconstructed outlines of Palaeolake Olduvai in different phases of extension are from Ashley et al. (2014).

(Tanzania). The latter two species have been informally termed Palaeoafrikan *Crocodylus* by Cossette et al. (2020).

In this paper, we describe a new partial cranium of crocodile collected from Olduvai Gorge sediments referred to Bed I, cropping out at DK East site. This specimen serves as a starting point for reevaluating some anatomical features of *C. anthropophagus* and to rearrange the phylogenetic relationships with other members of its genus.

Olduvai Gorge: a brief overview. Olduvai Gorge is a long valley incised by a seasonal river in the south-eastern margin of the Serengeti Plain, northern Tanzania. The rocks that crop out in the Gorge form an almost 100-m thick sedimentary sequence of lacustrine, alluvial, and aeolian deposits spanning the last 2 Ma (Fig. 1). These deposits lie on a lava unit and are interbedded by several tuff layers forming prominent marker units (Hay 1976).

From bottom to top, the Olduvai succession is classically divided into Bed I, Bed II, Bed III, Bed IV, Masek Beds, Ndtu Beds, and Naisiusiu Beds (Hay 1976). Recent research by the Olduvai Gorge Coring Project (OGCP) focused on four boreholes drilled into the Olduvai Basin depocentre and put into light about 135 m of previously unknown deposits beneath Bed I (Stanistreet et al. 2020a; Njau et al. 2021). These data were used in reconstructing stratigraphy and palaeoenvironment of a fan-delta originated by the nearby Ngorongoro Volcano (Ngorongoro Formation), and of an underlying fluvio-lacustrine non-volcaniclastic unit (Naivor Soit Formation). The authors also recognized disconformities between nearly all major surface units (Beds I, II, III, IV, Masek and Ndtu Beds), providing useful correlative boundaries of the Olduvai sequence (Stanistreet et al. 2020a). According to the latest core data, claystone and sandy claystone facies associations forming Bed I accumulated at the

bottom of Palaeolake Olduvai (Fig. 1) during the period of its maximum depth. Also the overlying Bed II-IV are dominated by claystone and sandy claystone facies associations. However, at least two pulses of fluvial deposition are recognized in Bed III, while lacustrine sediments are still prevalent in Bed II. A shallow lake was still present in the depocentre at the time of Bed IV formation (Hay 1976; Stanistreet et al. 2020a). The Masek Beds originate from Kerimasi Volcano and are made up of a mudflow-dominated fan-delta that entered the still extant Palaeolake Olduvai, whereas the Ndutu Beds facies association comprises aeolian sediments marked by phases of calcrete formation (Hay 1976; Stanistreet et al. 2020a).

Olduvai is recognized as one of the most important palaeontological and archaeological sites in the world thanks to the outstanding record of fossils and stone tools found within secure geological contexts, which offers a clear glimpse of human evolution in the context of East African environmental changes throughout the Pleistocene. Discoveries in the Gorge began more than a century ago by German researchers (e.g., Reck 1914), but much of the fame of the site is due to more than four decades of work of Drs. Louis and Mary Leakey at Olduvai. The discovery of holotype specimens of *Paranthropus boisei* (aka *Zinjanthropus*) and *Homo habilis* are among the first early hominin fossils to be found in Eastern Africa and became the most significant finds for understanding the evolution of our ancestors (Leakey 1959; Leakey et al. 1964; Wood 2011; Blumenshine et al. 2012). Numerous international research projects have collected fossils and stone artifacts since the early twentieth century at Olduvai Gorge, and several are still underway, including the Tanzania Human Origins Research (THOR) project. This Italian-Tanzanian project aims at surveying, excavating, and studying different palaeontological and archaeological contexts in Olduvai (Cherin et al. 2016), but widens its horizons also towards other Tanzanian palaeoanthropological sites, such as Laetoli (Masao et al. 2016).

MATERIALS AND METHODS

In 2016, the THOR team excavated a new trench at site DK East (DK-E), located about 500 m East from the main Leakey DK trenches (Leakey 1971; Fig. 2). The new trench exposed a 5 m-thick sedimentary succession situated between the Bed I Basalt at the bot-

tom and Tuff IB at the top. In order to document and study the stratigraphic context, 24 geological samples –numbered BS1 to BS24 from the bottom upwards– were collected from the new trench. For each sample, colour (on dry sample), texture, and lithology were reported following Catt (1990) and Munsell® Soil Colour Chart.

The crocodile fossil described in this paper was discovered on September 1, 2016 by fossil hunter Agustino Venance during an annular solar eclipse and was therefore nicknamed “Black Sun” (BS). Following the field numbering of the THOR project and considering the specimen nickname, it is here referred to as THOR16_100BS, and the newly excavated trench is named BS Trench (Fig. 2).

Trench and fossil locations and geological sequence were recorded by GPS, photos and field drawings. The cranium was carefully removed from the site and transported to the Leakey Camp for preparation, which required a long and complex work as the specimen was almost completely included in a very compact carbonate concretion. The tools used to remove embedding rock included small hammers and chisels for larger portions of sediment, stainless-steel dentist tools and scalpels for removing small portions of sediment, and a compressed-air vibrating cutter for high-precision work. After preparation, it resulted that the specimen comprises five cranial fragments, which were numbered as THOR16_100BS1–5 from the front to the back. The first two fragments (THOR16_100BS1-2) and the last three (THOR16_100BS3-4-5) conjoin and can be refitted.

To facilitate the comparative analysis, 3D models of THOR16_100BS and of a cranium of extant *C. niloticus* kept at Leakey Camp were created using the Structure from Motion photogrammetry method. Photographic acquisition and data processing were carried out at Leakey Camp in August 2017.

The photographic sets used for the five fossil fragments and modern specimen included a Canon 500D camera equipped with an 18-55 mm zoom lens and tripod stand, a neutral-colour background and two 10 cm rulers (for the five THOR16_100BS fragments) or two 20 cm rulers (for the *C. niloticus* cranium), used to scale the models during post-processing. In order to ensure that the final 3D model was complete in every detail, all parts of each fragment were acquired according to the following procedure. A fragment and the two rulers were set on the stage and several photos were shot by placing the camera in different positions, 360° around the stage. Then the rulers were removed and the fragment was turned so that parts previously covered were exposed, and another series of photos was shot following the aforementioned method. This procedure was repeated until the fragment was completely covered, the final number of photos per fragment varying between 83 and 160 depending on its morphological complexity. The pictures were initially processed under Adobe Lightroom software to improve the graphic rendering of the 3D model textures by applying automatic correction of chromatic aberration and by lightening shadows and darkening lights, which allows to have less evident shadows in the final texture. Then the pictures were processed under Agisoft Photoscan software. The first step –i.e., photo alignment– was always successful in aligning all pictures at the first trial. Scaling was carried out by applying four markers, one at each of the two ends of the rulers. The markers of each ruler were transformed into scalebars with associated metric values, and the software used them to scale the objects by applying also the bundle adjustment, which corrects for small misalignments resulting from automatic alignment. Measurement redundancy (in fact a single scale bar would have been enough to scale the object) was used to calculate the reprojection error, which did not exceed more than 1 mm and was therefore considered acceptable. The following processing steps created the dense point cloud and the meshed three-dimensional surface of the pieces. Finally, texture was applied to the 3D models to associate three-dimensional data with material and chromatic characteristics. Values derived from each

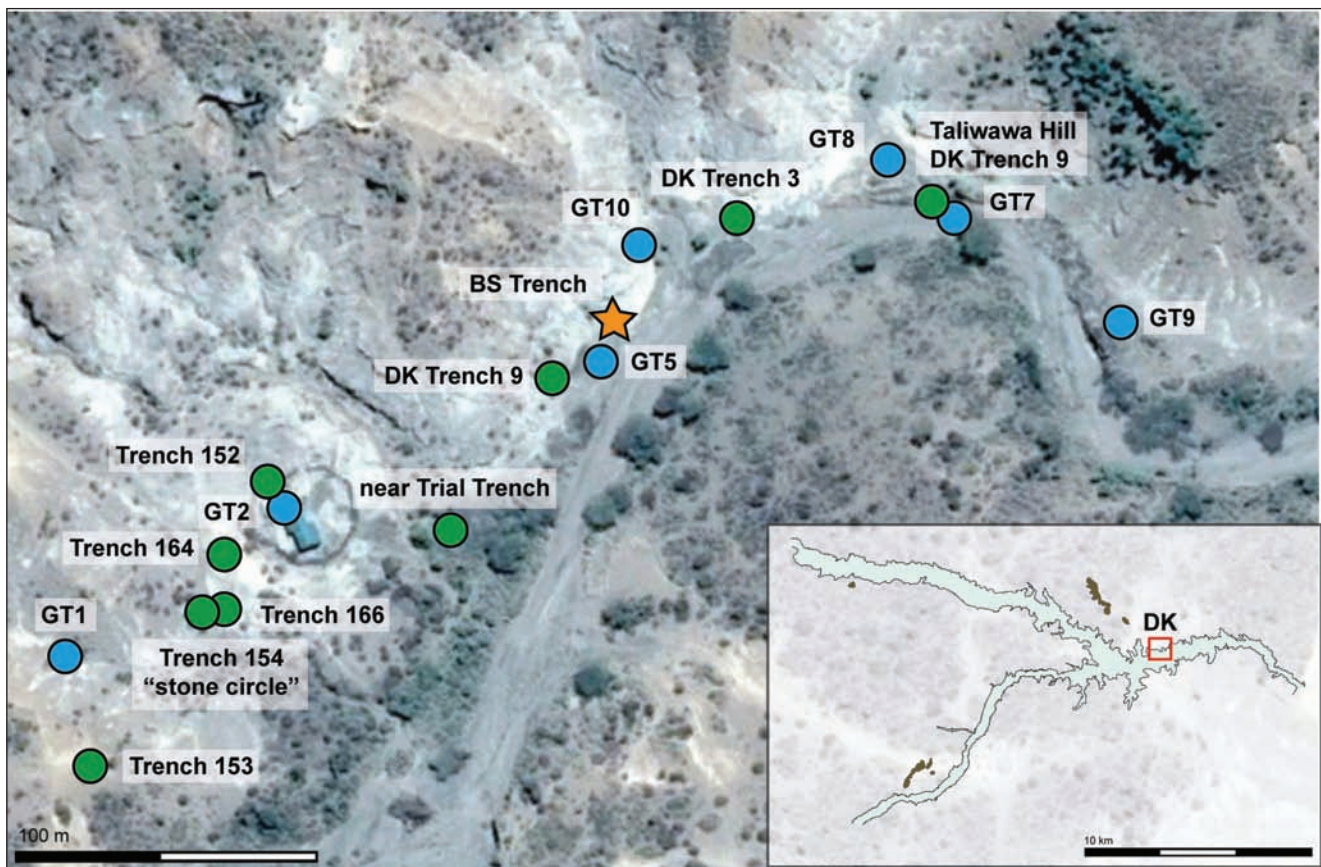


Fig. 2 - Google Earth map showing the position of the main trenches excavated in the Olduvai DK area over the years. Blue circles: Geo-Trenches by Ashley et al. (2016). Green circles: Trenches by Stanistreet et al. (2018), who also re-exhumed some trenches by Masao et al. (2013). The star shows the position of BS Trench.

processing phase (number of photographs, number of markers, total reprojection error in millimetres, number of tie points and points of the dense cloud, number of polygons in the 3D models and size of the texture in pixel) are listed in Table 1 and show the high level of geometric definition and photorealistic resolution achieved.

3D models were analysed and measured with Avizo 7 and MeshLab 2020.07, while virtual restoration and final editing process of the images (i.e., colouring of the duplicated portions) were carried out under ZBrush 4R6. Using the complete 3D cranium of *C. niloticus* as reference, the preserved left portions of Black Sun were mirrored and manually reconnected matching the complementary margins of the bones. Despite the lack of the median

portion of the rostrum, the very good refitting of the fragments allowed to obtain an improved 3D model of the fossil, which was subsequently used to estimate cranial and body size of Black Sun. A short 3D animation of the restored cranium was built by ZBrush (see Supplementary video 1). The 3D models of THOR16_100BS are available for download at <https://www.morphosource.org/projects/000362057?locale=en>.

Direct comparison was carried out using the aforementioned extant *C. niloticus* specimen, whereas additional data on extant and extinct African crocodiles refer to literature by Brochu (2000), Delfino et al. (2004, 2018, 2020, 2021), Brochu et al. (2010), Brochu & Storrs (2012).

ID	Pictures (number)	Markers (number)	Total reprojection error (mm)	Tie points (points)	Dense clouds (points)	3D models (polygons)	Texture resolution (pixel)
THOR16_100BS1	160	4 (2 x 2 scale bars)	0.14	80877	4301095	9253432	4096 x 4096
THOR16_100BS2	129	4 (2 x 2 scale bars)	0.10	72121	6388637	13643402	4096 x 4096
THOR16_100BS3	83	4 (2 x 2 scale bars)	0.11	49556	3838590	8457902	4096 x 4096
THOR16_100BS4	130	4 (2 x 2 scale bars)	0.03	82126	7075201	15696918	4096 x 4096
THOR16_100BS5	87	4 (2 x 2 scale bars)	0.02	53408	4351122	9382948	4096 x 4096
<i>C. niloticus</i>	142	4 (2 x 2 scale bars)	0.27	32827	1691220	3992118	4096 x 4096

Tab. 1 - Technical specifications of the photogrammetric process.

GEOLOGICAL CONTEXT

Olduvai DK site. Douglass Korongo (DK), also known as Archaeological site number 22 (Leakey 1971) and Geolocality 13 (Hay 1976), is located in the eastern part of the Olduvai basin on the North bank of the Olduvai River, approximately 2.5 km East of the junction between Main Gorge and Side Gorge (Fig. 1). DK is one of the most famous sites in Olduvai Gorge, the oldest site in the eastern basin (at the base of Bed I; see below), and one of the earliest studied by Mary Leakey (Masao et al. 2013). Moreover, it has been described as one of the richest sites in terms of palaeontological and archaeological content, as it yielded hundreds of stone tools and faunal remains over the decades, including some outstanding hominin fossils such as the nearly complete cranium OH24 referred to *Homo habilis* (Leakey 1971; Leakey et al. 1971). The DK palaeoenvironment is reconstructed as a wetland characterized by abundant grasses and a diversity of potentially edible plants, like papyrus rhizomes (Hay 1976; Albert et al. 2015; Ashley et al. 2016). Evidence of hominin activities is represented not only by archaeological artifacts but also by frequent modification traces on faunal remains (Potts 1984; Reti 2016).

In the early 1960s, Mary Leakey carried out the first research at the site, excavating the so-called “Leakey DK trenches” (DKI, DKIA or “Stone Circle”, DKIB, IC, MK, and Trial Trench; Leakey 1971). She discovered a high concentration of fossils and artefacts in the stratigraphic interval between Bed I Basalt and Tuff IB, including an enigmatic circular arrangement of stones, about 5 m wide. Leakey (1971) considered the DK palaeosurface as an “occupation floor” and the “stone circle” as the remains of a shelter built by hominins, although this reconstruction was disputed by other researchers that interpreted the circle as a natural formation (Potts 1984; Njau 2012). Masao et al. (2013) excavated nine more trenches (DK trenches II–X) eastward of Mary Leakey’s ones, i.e., in DK-E area (Fig. 2). These yielded more than a thousand faunal remains mostly referred to Bovidae (over 40%) and Crocodylidae (ca. 14%). Ashley et al. (2016) excavated ten 1 m-wide trenches in a 450 m exposure along the DK classic site and DK-E (Geo-Trenches 1–10; Fig. 2). Stanistreet et al. (2018) analysed three trenches (152, 153, and 154) adjacent to the Leakey DK trenches along a NE-SW line (Fig. 2) and four

trenches (160, 161, 164, and 166) along a perpendicular transect, towards NW-SE. They also re-exhumed the Trial Trench, DK trench IX, DK trench III, and DK trench II (Taliwawa Hill). This latter work allowed to reconstruct a new sequence stratigraphy context for DK based on the identification of five “Lake-parasequence” (P1 to P5) boundaries, and to correlate the stratigraphic position of Mary Leakey’s “occupation floor” along the site.

The age of the DK stratigraphic succession is well constrained by those of Bed I Basalt at the bottom and of Tuff IB at the top. The former was originated by Ngorongoro Volcano and stratigraphically separates the Lower and Upper Bed I (Stanistreet et al. 2020a). Among the Bed I marker tuffs (Tuffs IA–IF; Hay 1976), Tuff IB is well recognizable in DK and is often used as a marker horizon for stratigraphic correlations (e.g., Stanistreet et al. 2018). Tuff IB is a vitric trachyte tuff that was deposited by one of the explosive eruptive phases of Olmoti Volcano and comprises ash-flow tuff, both primary and reworked (including pumice bombs and lapilli) and widespread air-flow tuff (Leakey 1971; Hay 1976; McHenry 2004). $^{40}\text{Ar}/^{39}\text{Ar}$ dating of the Bed I Basalt and Tuff IB yielded ages of 1.8777 ± 0.013 Ma and 1.848 ± 0.003 Ma, respectively. However, recent data from precessional cycle periodicity suggested that the Bed I Basalt might be older (~ 1.94 Ma; Stanistreet et al. 2020b).

Description of BS Trench. The BS Trench exposes a section spanning for about 5.2 m between the top of Bed I Basalt and Tuff IB (Fig. 3a). Based on previously published maps, the BS Trench is located in close proximity of Geo-Trench 5 of Ashley et al. (2016), that is, between Trial Trench and DK Trench X (Leakey 1971; Masao et al. 2013; Stanistreet et al. 2018; Fig. 2). The eye-scale characteristics of the section obtained by observation of the 24 collected samples are reported in Table 2. The different portions of the section are detailed hereafter following their analogies with facies and/or significant stratigraphic intervals described in DK by Stanistreet et al. (2018) and other authors.

The interval between 0.00 and 0.90 m (samples BS1–BS8) can be referred to the “fluvio-deltaic sandstone and heterolithic facies association (i.e., volcanoclastic sandstone, claystone interbedded with thin sandstones)” of Stanistreet et al. (2018), which probably formed in shallow ephemeral braid-

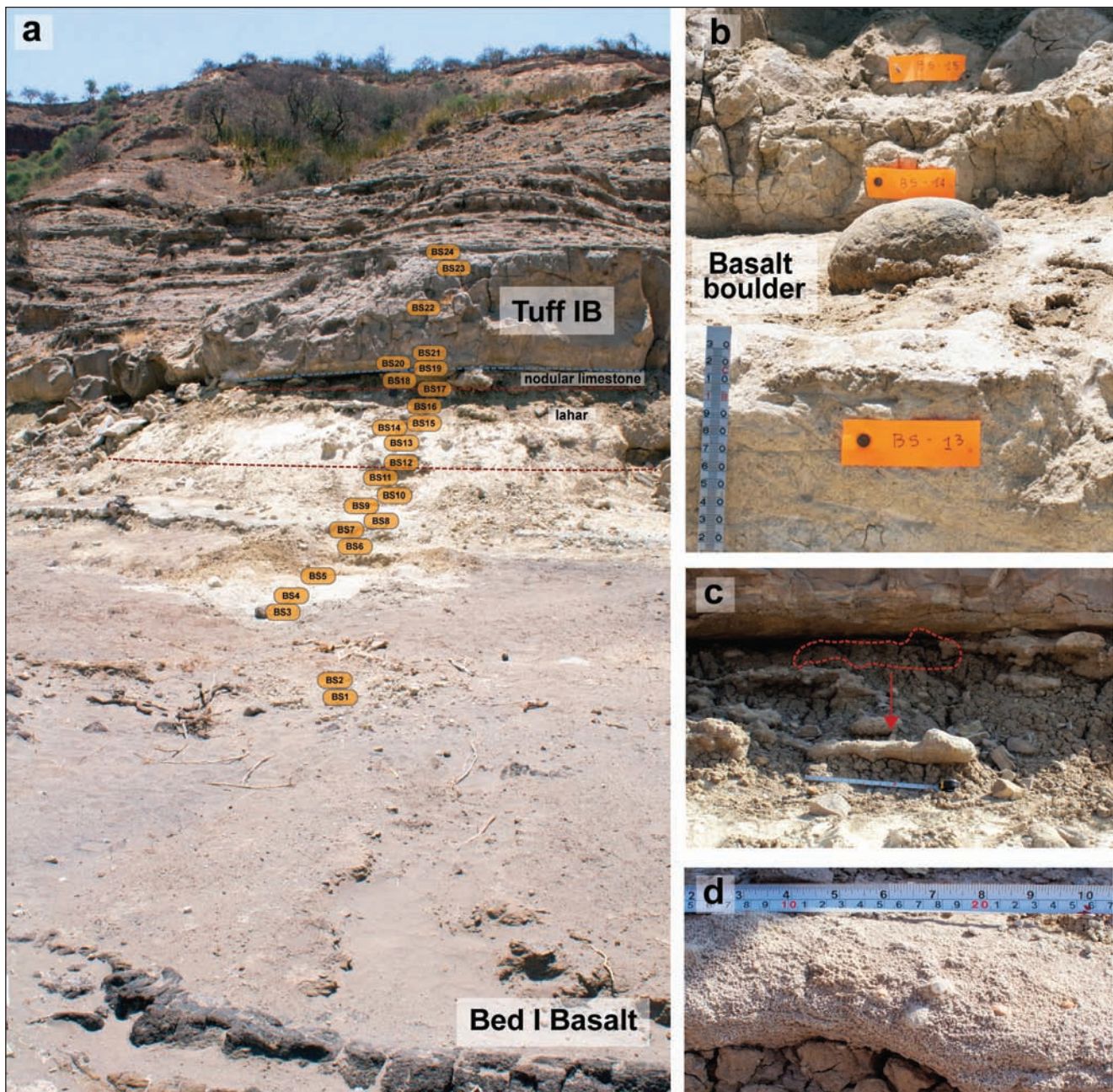


Fig. 3 - BS Trench at Olduvai DK-E. a) Overall view of the trench, which exposes a section spanning for about 5.2 m between the top of Bed I Basalt and Tuff IB; the position of the 24 collected samples and the contact between the lahar (*sensu* Stanistreet et al. 2018) and the overlying nodular limestone are marked up. b) Detail of the interval between samples BS13 and BS15 showing a basalt boulder. c) Detail of the middle part of the outcrop in which Black Sun (THOR16_100BS) was found; the cranium was embedded in a concretion block lying ca. 60 cm below its original position, where a detachment niche was identifiable. d) Detail of the block of nodular limestone containing the specimen; some teeth are visible coming out from the concretion block.

ed fluvial channels.

The interval between 0.90 and 1.45 m (samples BS9–BS11) can be referred to the “lacustrine claystone facies association (waxy claystone, sandy waxy claystone)” of Stanistreet et al. (2018), correlative to the “brown clay” of Leakey (1971), which formed as suspension fallout in a saline alkaline lake palaeoenvironment.

The interval between 1.45 and 2.60 m (samples BS12–BS17) can be referred to the “mass flow diamictites (volcaniclastic diamictite, sandy volcaniclastic diamictite: clay-rich matrix-supported conglomerates and sandstones)” of Stanistreet et al. (2018). The term “diamictite” is used by Stanistreet et al. (2018) following Flint et al. (1960) to indicate generically a poorly-sorted sedimentary rock with

Sample	Colour code	Colour name	Texture	Aggregation	Other features
BS1	5Y8/2	Pale yellow	Sandy loam	Massive	Some small Mn mottles
BS2	2.5Y 7/1	Light gray	Loam (few very fine sand)	Massive	Very few Mn mottles
BS3	2.5Y6/3	Light yellowish brown	Loamy sand (very fine sand)	Massive	
BS4	2.5Y6/3	Light yellowish brown	Loamy sand (very fine to medium sand)	Massive	
BS5	5Y7/4-6/4	Pale yellow-pale olive	Sandy clay loam	Massive	Whitish mottles (CaCO ₃)
BS6	5Y7/3-6/3	Pale yellow-pale olive	Sandy clay loam	Medium developed blocky	Whitish mottles (CaCO ₃)
BS7	5YR7/1	Light gray	Loamy sand (very fine sand)	Massive	Laminated (1-3 mm layers); few cracks
BS8	2.5Y8/2	Pale yellow	Loamy sand (very fine sand)	Massive	
BS9	5Y5/1	Gray	Sandy loam	Poorly developed blocky	Whitish mottles (CaCO ₃)
BS10	2.5Y7/2	Light gray	Loamy sand (fine sand)	Loose	Whitish mottles (CaCO ₃)
BS11	5Y4/3-4-4	Olive	Very fine sandy clay	Poorly developed blocky	Whitish mottles (CaCO ₃)
BS12	2.5Y8/2	Pale yellow	Sandy loam (very fine to fine sand)	Loose	
BS13	2.5Y8/2	Pale yellow	Sandy loam (very fine to fine sand)	Loose	
BS14	2.5Y7/4	Pale yellow	Sandy loam (very fine to medium sand)	Very poorly developed blocky	Whitish mottles (CaCO ₃); cracks
BS15	5Y7/2	Light gray	Clay with some sand (very fine to medium sand)	Massive	Whitish mottles (CaCO ₃)
BS16	5Y5/3	Olive	Clay with some sand (very fine to medium sand)	Massive	Whitish mottles (CaCO ₃); whitish fossil bone fragments
BS17	5Y4/3-4-4	Olive	Clay	Medium developed blocky	Whitish mottles (CaCO ₃); quartz grains
BS18	5Y7/2	Light gray	Sandy clay (very fine to medium sand)	Massive	CaCO ₃ pebbles and quartz grains
BS19	5Y4/2	Olive	Clay	Medium developed blocky	Laminated (very fine layers); few Mn and CaCO ₃ mottles
BS20	5Y8/2	Pale yellow	Sandy loam (few very fine sand)	Massive	Feldspar crystals
BS21	2.5Y8/1-7/1	White-light gray	Sandy loam (very fine to fine sand)	Massive	
BS22	2.5Y7/1	Light gray	Loamy sand (medium sand)	Massive	
BS23	2.5Y7/1	Light gray	Loamy sand (very fine sand)	Massive	Few whitish mottles (CaCO ₃)
BS24	10YR8/2	Very pale brown	Unsorted conglomerate	Poorly developed blocky	Clasts up to 1-2 cm of pumice, quartzite, and other rocks

Tab. 2 - Eye-scale characteristics of the geological samples from BS Trench, DK-E site, Olduvai Gorge. The position of the samples is shown in Fig. 3a.

very heterogeneous particle sizes. This portion of the sequence correlates with the “buff-yellow sandy clay” and “gray-brown sandy clay” of Leakey (1971) and formed as a volcanoclastic mudflow (lahar) originated by Ngorongoro Volcano, which rapidly buried the DK main archaeological horizon, i.e., Leakey’s (1971) “occupation floor” (Stanistreet et al. 2018). Basalt pebbles and boulders were identified within this interval in BS Trench (Fig. 3b), in agreement with Stanistreet et al. (2018) descriptions.

The interval between 2.60 and 2.80 m (sample BS18) can be referred to the “nodular calcareous paedogenic and groundwater precipitates (micritic nodular to spherulitic nodular limestone)” of Stanistreet et al. (2018). The crocodile specimen described in this paper (THOR16_100BS) was found in this layer (actually, the carbonate concretion block that contained the cranium was found about 60 cm below, because it had detached from the original position, of which however a clear detachment niche was identifiable; Fig. 3c). Similarly, based on original field descriptions (Leakey et al. 1971), it is very likely that the cranium of *H. habilis* OH24 was collected from the same layer, but further East (i.e., close to Taliwawa Hill Trench II; Masao et al. 2013; Stanistreet et al. 2018; Fig. 2). This layer is easily identifiable in the field as a massive limestone very rich in sub-spherical

carbonate nodules (Fig. 3d), quartzite artifacts, and isolated crocodile teeth (Fig. 4), as also pointed out by Masao et al. (2013). The base of the layer exhibits a heavily gullied surface that undercuts the underlying olive-coloured claystone, similarly to what is described in DK Trench IX by Stanistreet et al. (2018). Ashley et al. (2020) studied the distribution, depositional genesis, lithology, petrography, and geochemistry of freshwater carbonates traceable in Upper Bed I (ca. 1.8 Ma) throughout Olduvai Gorge. The authors recognized five carbonate lithologies, four of which deposited in a catena-like pattern over connected palaeoenvironments (spring, wetland, freshwater lake/pond, and saline playa lake). The fifth carbonate lithology, i.e., the nodular limestone that can also be found in BS Trench, formed by pedogenesis in topographically higher areas of the basin (e.g., the DK Horst; Stollhofen & Stanistreet 2012), where “surface water seeped into clayey sediments, mixed with groundwater and became concentrated at nucleation sites to form nodular limestone” (Ashley et al. 2020: 345). The recognition of other paedogenetic features (e.g., desiccation cracks, mottles, and root traces) in the same deposit (Ashley et al. 2020) suggests that it formed in a low-stand phase of Palaeolake Olduvai in the DK area, confirming that the lake was subject to a seasonal changing regime (Ashley et al. 2016).

Fig. 4 - Isolated crocodile teeth (THOR16_16) recovered in Olduvai DK-E from the same layer as the cranium THOR16_100BS. Scale bar: 3 cm.



The interval between 2.80 and 5.20 m (samples BS19–BS24) is entirely occupied by Tuff IB. As Hay (1976) reported for Geolocality 13 (aka DK site), Tuff IB is a vitric trachyandesite tuff that comprises a thin olive-coloured ash-fall stratum (sample BS19) overlain by an ash-flow deposit up to 4 m thick (ca. 2 m in our case; samples BS20–BS23) containing abundant pumice lapilli (0.5 to 2.5 cm diameter in BS Trench). The unsorted conglomerate identified at the top of the section is reported by Hay (1976) as a stream-worked ash-flow deposit.

SYSTEMATIC PALAEOLOGY

Crocodylia Gmelin, 1788

Crocodylidae Cuvier, 1807

Crocodylus Laurenti, 1768

Crocodylus anthropophagus Brochu et al., 2010

Figs 5-6, Supplementary video 1

Referred material: THOR16_100BS, partial cranium (partial rostrum: fragments THOR16_100BS1 and THOR16_100BS2; nearly complete neurocranium: fragments THOR16_100BS3, THOR16_100BS4, and THOR16_100BS5), stored in the Leakey Camp, Olduvai Gorge (Tanzania).

Emended diagnosis: *Crocodylus* with a prominent triangular projection (“horn”) at the posterolateral corner of each squamosal dorsal to otic aperture at maturity; projection is subtriangular in lateral view and has discrete boundaries mediolaterally and anteroposteriorly, with shorter sub-vertical anterodorsal margin and longer gently sloping posterodorsal surface. Pair of crests on rostrum corresponding to the maxillary-nasal sutures. Maxillary ramus of ectopterygoid may not be forked, though expression of the cleft varies intraspecifically in most modern *Crocodylus*. External naris opens anterodorsally rather than dorsally. Lacks the elongate preorbital crest typical of Indo-Pacific *Crocodylus*, and lacks the median rostral boss diagnostic for Neotropical *Crocodylus* and African *C. chechibaii*. Skull table with convex lateral margins, which continue posteriorly into well-developed posterolateral squamosal rami along the paraoccipital processes of exoccipitals (modified from Brochu et al. 2010).

Description. The five fragments together form an incomplete cranium, which shows an evident diagenetic dorsoventral crushing (Figs 5-6). The best preserved and least deformed part is the dorsal portion of the neurocranium, including the skull table. The right side of the cranium is almost complete, as it lacks only part of the jugal and prefrontal, the posterior part of the maxilla and of the nasal. The lacrimals, palatines, pterygoids, and ectopterygoids are missing in both sides. Starting from the preserved parts, we virtually reconstructed the whole cranium, of which we can estimate a maximal width of 27 cm and a dorsal length of about 50 cm. However, the latter measurement should be considered with caution due to the lack of the median portion of the rostrum.

THOR16_100BS1 includes most of the right premaxilla, whereas THOR16_100BS2 includes the most posterior portion of the right premaxilla, the anterior part of the right maxilla, and the anterior half of the right nasal. The two fragments are significantly flattened dorsoventrally. They perfectly fit each other and are described below as a single unit. In dorsal view, the premaxilla has a rounded lateral margin. The external naris has a semi-circular outline and it opens flush with the dorsal surface of the premaxilla, which shows a shallow notch posterolaterally to the naris. The anterior tip of the right nasal is not preserved so its relationship with the external naris is not identifiable. The premaxillary-maxillary suture is faintly visible at the anteromedial corner of THOR16_100BS2 and seems rather straight. The palatal process of the premaxilla is not preserved (except for a small splinter of bone displaced from its anatomical position, which was intentionally left attached close to the third and fourth teeth during the preparation of the specimen).

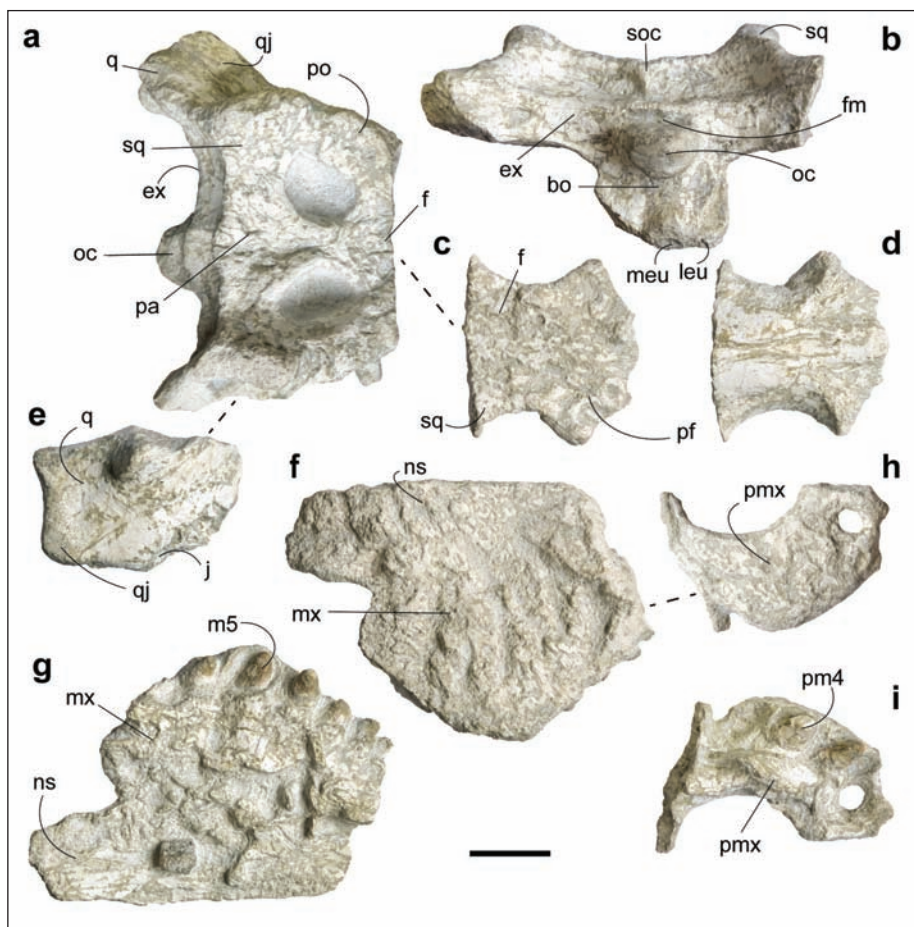


Fig. 5 - Cranium Black Sun (THOR16_100BS) from Olduvai DK-E. a-b) Specimen THOR16_100BS4 in dorsal (a) and posterior (b) views. c-d) Specimen THOR16_100BS3 in dorsal (c) and ventral (d) views. e) Specimen THOR16_100BS5 in dorsal view. f-g) Specimen THOR16_100BS2 in dorsal (f) and ventral (g) views. h-i) Specimen THOR16_100BS1 in dorsal (h) and ventral (i) views. Abbreviations: bo, basioccipital; ex, exoccipital; f, frontal; fm, foramen magnum; j, jugal; leu, lateral Eustachian foramen; me, median Eustachian foramen; m5, fifth maxillary tooth; mx, maxilla; ns, nasal; oc, occipital condyle; pa, parietal; pf, prefrontal; pm4, fourth premaxillary tooth; pmx, premaxilla; po, postorbital; q, quadrate; qj, quadratojugal; soc, supraoccipital; sq, squamosal. The dashed lines indicate the contacts between joining fragments. Scale bar: 5 cm.

The dorsal surface of the maxilla is flat, but this morphology may have been exaggerated by the diagenetic flattening. The maxillary-nasal suture corresponds to a low crest-like step as the nasal is slightly elevated over the dorsal surface of the maxilla. On the ventral side, the palatine process of the maxilla is missing and only preserved as isolated bone splinters. A small cubic fragment of quartzite was left attached on the ventral surface of the specimen, close to the contact between the maxilla and nasal. In medial view, the internasal suture surface is slightly convex dorsally and is thicker in the posterior part than in the anterior.

The premaxilla bears five alveoli. The third and fourth teeth are preserved and are quite massive, with the fourth being larger than the third. The latter is more elongated and pointed than the first. The first and second alveoli are preserved only in their posterior margins. The first is smaller than the second. The fifth alveolus is wide and relatively smaller than the fourth. There is a diastema between the second and third alveoli. A wide hole due to serration with a dentary tooth opens on the premaxilla medially to the third premaxillary tooth. Eight alveoli, the

first six hosting teeth, are present in the preserved portion of the maxilla. The first and second teeth are relatively small. The third is broken but appears larger than the latter two. Teeth four to six are complete, robust, and conical. The alveolus of the fifth maxillary tooth is the largest, although only the tip of the tooth itself is visible as it was erupting. The seventh and eighth alveoli are placed medially to the sixth tooth, that is, the maxillary tooth row is oriented in anterolateral to posteromedial direction posterior to the fifth maxillary tooth. In all preserved premaxillary and maxillary teeth, the enamel surface is ornamented with a fluted pattern and strong mesial and distal un-serrated carinae are present.

Looking at the anterior portion of the rostrum, the lateral margin at the contact between the premaxilla and maxilla is gently inflated, giving to the rostrum an overall hourglass shape. In lateral view, the dorsal margin of the premaxilla is slightly concave and anterodorsally inclined in the anterior portion. Due to deformation, the rostral portion posterior to the external naris is concave ventrally, preventing the evaluation of the original orientation of the external nares.

THOR16_100BS3, THOR16_100BS4, and THOR16_100BS5 can be merged together and form most of the posterodorsal and posterior parts of the cranium. THOR16_100BS3 includes the posterior portions of the left and right prefrontals, frontals, and the anterior extremities of the squamosals. THOR16_100BS4 includes the whole skull table, the occipital region, and the dorsal wall of the braincase. THOR16_100BS5 completes the right squamosal with its posterolateral part and also includes the right quadrate, the quadratojugal, and a fragment of the jugal.

The prefrontals and frontals form the anteromedial and medial margins of the orbits, respectively. The dorsal surface of the prefrontal is medially flat, but it rises laterally to form a discrete knob-like process along the orbit margin. A shallow notch separates this process from the marked ridge of the frontal which delimits the orbit medially. In anterior view, the prefrontals are separated by a well-developed frontal ridge. In lateral view, the portions of prefrontal and frontal bordering the orbit are upturned. The dorsal frontal surface between the orbits is slightly concave. The frontoparietal suture is triangular in shape, with the posterior vertex extending far backwards until it wedges between the supratemporal fenestrae. In ventral view, the prefrontals are markedly concave. The anterior process of the frontal is well visible as a rectangular projection enclosed between the prefrontals. The posteroventral surface of the frontals is swollen, with a deep groove separating them. No prefrontal pillars are preserved.

In dorsal view, the skull table is very well preserved and appears relatively wide. Its lateral margins are laterally convex and continue posteriorly into significant posterolateral squamosal rami along the paraoccipital processes of exoccipitals. The postorbital forms the anterolateral margin of the supratemporal fenestra but the sutures between this bone and the surrounding ones (frontal, parietal, and squamosal) are not visible on both sides. On the right, the postorbital bar is preserved in its dorsal portion and is relatively slender. The squamosal delimits the supratemporal fenestra along its posterolateral margin. The dorsolateral part of the squamosal is largely occupied by a prominent horn-like projection. In lateral view, this horn is subtriangular in shape, with a steep anterodorsal margin and a more gently sloping posterodorsal

one. The angle between these two margins is about 90°. In posterior view, the same horn exhibits a nearly flat dorsal edge and subvertical lateral and medial margins, thus being clearly individualized from the rest of the squamosal. In lateral view, the squamosal groove is very deep, straight, parallel to the longitudinal axis of the cranium, and delimited by prominent dorsal and ventral rims. Posteriorly, the squamosal does not extend beyond the posterior extremity of the paraoccipital process of exoccipital.

In the middle of the skull table, the dorsal surface of the parietal is flat, with the exception of a deep sagittal groove running along the interparietal area between the supratemporal fenestrae. In ventral view, two oblique wide grooves developing posteriorly to the supratemporal fenestrae, can be interpreted as the left and right parietal recesses, respectively.

In posterior view, the occipital area is nearly complete but compressed dorsoventrally, so much that the foramen magnum is almost completely obliterated. In the dorsal part, the supraoccipital appears as a low and wide area, characterized by two deep fossae separated by a sagittal crest that thickens dorsally. The supraoccipital exposure on the skull table is very small and triangular in dorsal view. The same shows a slight sagittal inflection in posterior view. The exoccipital has a slightly concave posterior surface. The vagus foramen is well visible near the condyle on both sides, and opens in a triangular shallow depression. The other foramina on the exoccipital are obliterated. The basioccipital is partially preserved. The condyle is prominent and hemispherical in posterior view. The ventral part of the basioccipital is crossed by a strong sagittal crest, which culminates ventrally with a wide median Eustachian foramen. On the right side, laterally to the latter and at the same level, a smaller opening along the ventral margin of the basioccipital, is interpreted as the lateral Eustachian foramen. In lateral view, the basioccipital surface is markedly inclined in posteroventral direction. In ventral view, the basisphenoid is missing and its articulation surface with the basioccipital has the shape of a fluted, concave fan-like surface. At the anteroventral portion of this feature, the dorsal walls of the choanae are visible. The latter are not deeply notched and there is a slight evidence of a septum between them.

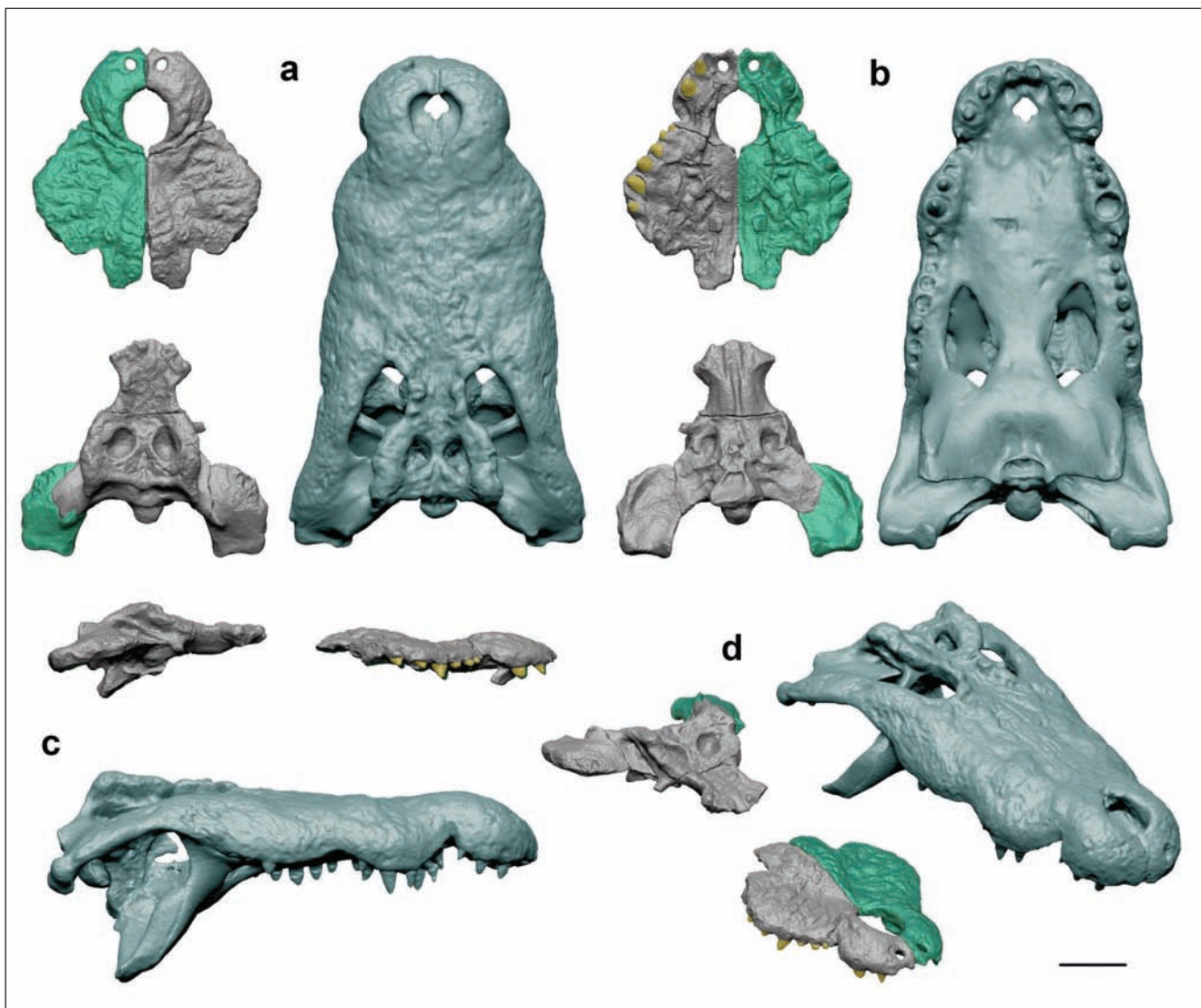
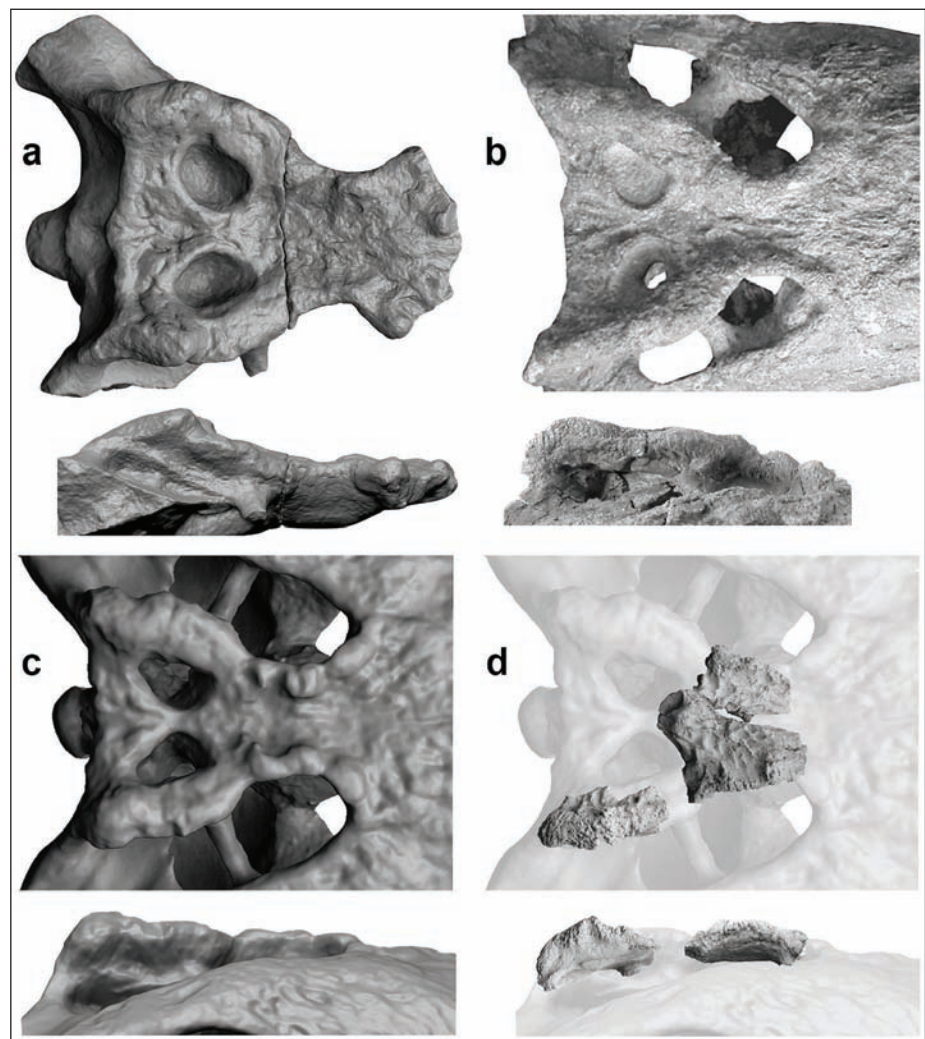


Fig. 6 - 3D models of Black Sun (THOR16_100BS) from Olduvai DK-E (left) compared with a cranium of extant *Crocodylus niloticus* (uncatalogued specimen kept at the Leakey Camp, Olduvai Gorge; right) in dorsal (a), ventral (b), right lateral (c), and oblique (d) views. Cloned and mirrored portions of Black Sun are highlighted in green. Scale bar: 10 cm.

The quadrate-quadratojugal complex has a sub-rectangular shape in dorsal view. The lateral margin of the quadratojugal is slightly convex, whereas the medial margin of the quadrate is slightly concave. In lateral view, the quadratojugal extends anteriorly through a crest-like process towards the superior angle of the infratemporal fenestra, contacting the postorbital bar (i.e., the quadrate does not participate in delimiting the infratemporal fenestra). In posterior view, the quadrate has an expanded medial hemicondyle, which is almost as wide as the lateral one. The dorsal and the ventral edges of the posterior face of the quadrate have a sinusoidal shape, with the ventral surface of the medial hemicondyle more prominent than the lateral hemicondyle.

Comparisons. The morphological features described above allow to undoubtedly refer THOR16_100BS to Crocodylidae. Comparisons are here limited to the four species of extinct and extant African species of *Crocodylus*, i.e., *C. anthropophagus*, *C. checciaii*, *C. niloticus*, and *C. thorbjarnarsoni* (*C. suchus* is not taken into consideration because it is currently considered as skeletally congruent with *C. niloticus*; Brochu & Storrs 2012). The extant *M. cataphractus* is excluded from our comparative analysis for a series of morphological differences with THOR16_100BS including the extremely elongated and slender rostrum and the dorsally placed lateral Eustachian foramina with respect to the median foramen; the latter character is also observed in the extant *O. tetraspis* and

Fig. 7 - Comparative morphology of the dorsal (top) and lateral (bottom) parts of the neurocranium in selected specimens of African crocodiles. a) Black Sun (THOR16_100BS) from Olduvai Gorge; b) *Crocodylus thorbjarnarsoni* (holotype KNM-ER 1683 at the top, KNM-KP 30604 at the bottom) from Lake Turkana Basin, Kenya (modified from Brochu & Storrs 2012); c) extant *Crocodylus niloticus* (uncatalogued specimen kept at the Leakey Camp, Olduvai Gorge); d) *Crocodylus anthropophagus* (holotype NNHM-OLD-1001) from Olduvai Gorge (modified from Brochu et al. 2010). Images are not scaled.



its Miocene relative *Rimasuchus lloydi* (Brochu 2000, 2007; Brochu & Storrs 2012), which are also not considered herein.

Despite the incomplete preservation of the new specimen from Olduvai, we can exclude its attribution to the late Miocene *C. checcchiai* because the latter is diagnosed by a flat posterolateral margin of the squamosal (Delfino et al. 2020). However, THOR16_100BS shares with *C. checcchiai* the quadratojugal anterior extension to form the superior angle of the infratemporal fenestra. One of the most noticeable characters of *C. checcchiai*, namely the presence of a medial rostral boss (Delfino et al. 2020), cannot be identified in our specimen due to the lacking of the median part of the nasals.

Black Sun differs from *C. thorbjarnarsoni* from the Plio-Pleistocene of the Turkana Basin in the morphology of the skull table (which has a more trapezoidal dorsal outline with anteriorly convergent lateral margins in *C. thorbjarnarsoni*) and in the presence of squamosal “horns” (which are

not well developed in *C. thorbjarnarsoni*). Moreover, although absolute dimensions are not useful diagnostic characters in crocodylians especially in the absence of large samples, it is worth mentioning that *C. thorbjarnarsoni* is characterised by markedly larger size. One of the largest known crania of this species (KNM-ER 1682) is about 85 cm in length (Brochu & Storrs 2012), thus exceeding the estimated length of THOR16_100BS of at least 30 cm. On the other hand, the Olduvai fossil shares a number of features with *C. thorbjarnarsoni*, including a broad and deep anterior rostrum, a prominent crest along the maxillary-nasal suture, a knob-like process on the prefrontal surface along the orbit margin, upturned squamosals, lateral and median Eustachian foramina at the same level, quadratojugal extending anteriorly to delimit the superior angle of the infratemporal fenestra (Fig. 7).

According to Brochu & Storrs (2012) *C. thorbjarnarsoni* shares several morphological features with *C. anthropophagus* from Olduvai Gorge, includ-

ing prefrontal knobs, upturned squamosals, broad and deep snouts, and anterodorsally oriented external nares. All these characters are also visible in THOR16_100BS with the exception of the last, which is difficult to assess due to deformation. In addition, the new specimen shows strong triangular squamosal “horns”, which are very similar to those reported in the diagnosis of *C. anthropophagus* (Brochu et al. 2010; Fig. 7). As in the latter species, THOR16_100BS exhibits a pair of crests on the rostrum corresponding to the maxillary-nasal sutures. No previous information on the morphology of the skull table in *C. anthropophagus* were available in the literature due to the incompleteness of the described Olduvai material (Brochu et al. 2010).

No differences in either size or general morphology are found between THOR16_100BS and *C. niloticus*. However, at a closer look, the new specimen shows much more prominent crests along the maxillary-nasal sutures, less developed crest at the lateral margins of frontals, larger and more rounded supraorbital fenestrae, convex lateral margins of the skull table which are connected to prominent posterolateral squamosal rami along the paraoccipital processes of exoccipitals (Fig. 7). Dorsal projections at the posterolateral corner of the squamosal are normally absent in *C. niloticus* and, when present, are not as prominently developed and more rounded in lateral view, with less discrete demarcations from the rest of the skull table (Brochu et al. 2010). Therefore, this region of the cranium of *C. niloticus* clearly differs from the morphology described in Black Sun. Similarly, prefrontal knobs may be present in *C. niloticus* but their expression is variable and are not as prominent as in the Olduvai specimen, which more closely resembles the condition of *C. thorbjarnarsoni* and *C. anthropophagus* (Brochu & Storrs 2012). Finally, differently from the condition seen in THOR16_100BS, the quadratojugal of *C. niloticus* does not extend to the superior angle of the infratemporal fenestra, which is instead formed by the quadrate (Brochu & Storrs 2012).

These comparisons allow confident referral of THOR16_100BS from DK-E to *C. anthropophagus*. The new cranium can therefore be added to the hypodigm of the species and allows us to expand our knowledge on its anatomy, since it retains some portions –such as the complete skull

table– not preserved in the material described so far by Brochu et al. (2010). The diagnosis of *C. anthropophagus* is then amended on the basis of these newly observed characters.

PHYLOGENETIC ANALYSIS

We performed a maximum parsimony analysis in TNT v. 1.5 software (Goloboff et al. 2008) based on the matrix of Cossette et al. (2020), in turn modified from that of Brochu & Storrs (2012). The matrix includes 35 taxa and 189 characters (Supplementary file 1). Character 158 was modified as follows, to accommodate the condition observed in *C. anthropophagus* (state 1):

Original character (Brochu & Storrs 2012): Mature skull table with broad curvature; short posterolateral squamosal rami along paraoccipital process (0) or with nearly horizontal sides; significant posterolateral squamosal rami along paraoccipital process (1).

Modified character (this paper): Mature skull table with broad curvature; short posterolateral squamosal rami along paraoccipital process (0) or with nearly horizontal or slightly curved sides; significant posterolateral squamosal rami along paraoccipital process (1).

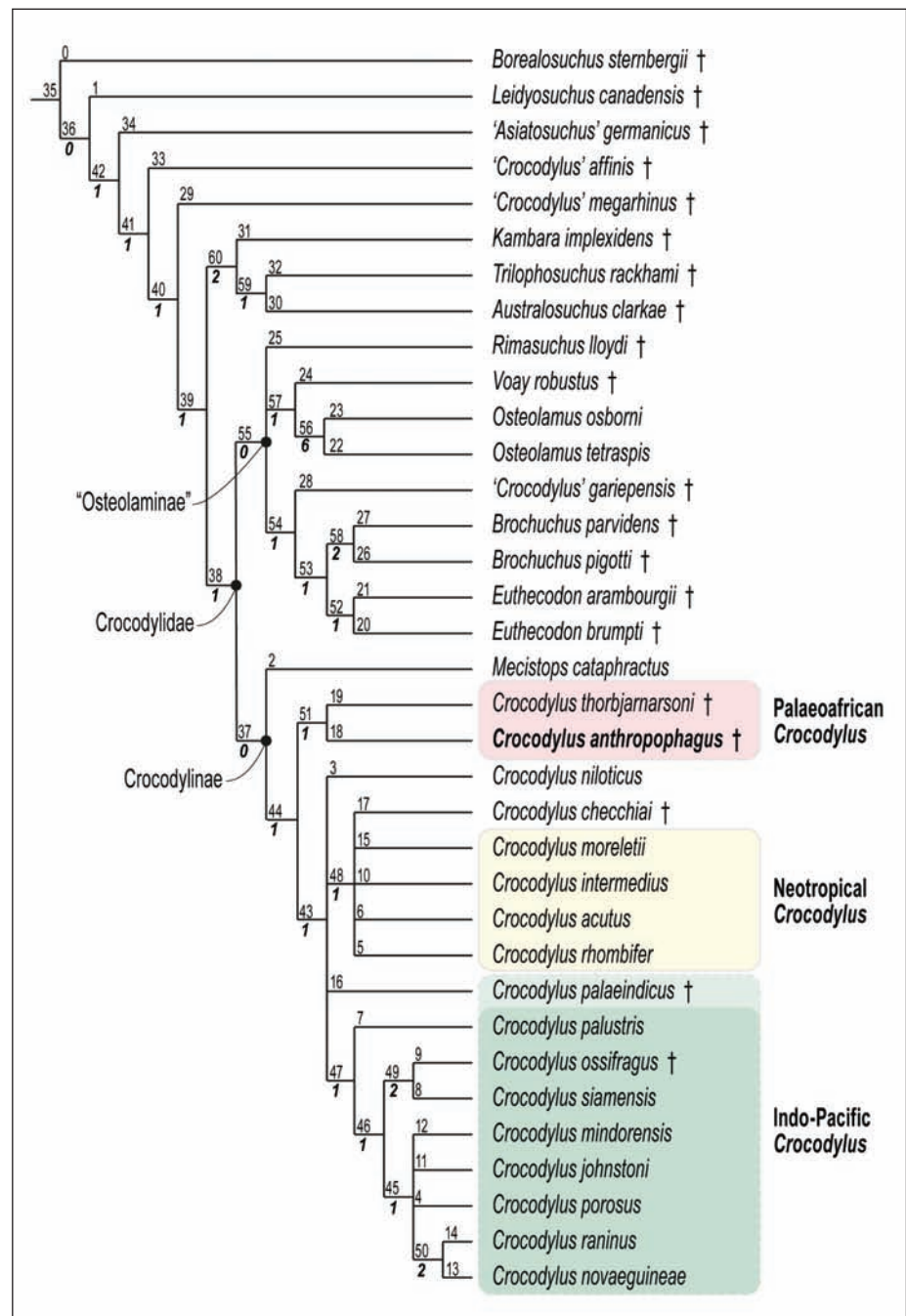
Borealosuchus sternbergii was set as outgroup. Characters were weighted equally, multistate characters were left unordered, and the analysis was conducted by “New Technology search” (default settings). We replaced the original coding of *C. checcchiai* (Brochu & Storrs 2012) with the most recent one by Delfino et al. (2020). The original coding of *C. anthropophagus* (Brochu & Storrs 2012) was modified as follows, on the basis of the characters observed on the new cranium THOR16_100BS:

Character 124: Posterior rim of internal choana not deeply notched (0) or deeply notched (1). Scoring modified from “?” to “0”. This character was not observable in the fragmentary original material of *C. anthropophagus* (Brochu et al. 2010).

Character 125: Internal choana not septate (0) or with septum that remains recessed within choana (1) or with septum that projects out of choana (2). Scoring modified from “?” to “1”. This character was not observable in the fragmentary original material of *C. anthropophagus* (Brochu et al. 2010).

Character 167: Parietal with recess communi-

Fig. 8 - Strict consensus tree showing the phylogenetic relationships between extant and extinct (†) crocodylians. Node numbers are indicated. Bremer support in bold italics below node numbers. The phylogenetic analysis is based on a matrix of 35 taxa and 189 characters updated from Cossette et al. (2020). Clade names are from Brochu (2020) and Cossette et al. (2020).



cating with pneumatic system (0) or solid, without recess (1). Scoring modified from “?” to “0”. This character was not observable in the fragmentary original material of *C. anthropophagus* (Brochu et al. 2010).

The phylogenetic analysis resulted in four equally parsimonious trees of 215 steps, consistency index of 0.600 and retention index of 0.717. The strict consensus tree is shown in Fig. 8.

The topology of our phylogenetic tree does not differ significantly from that of Cossette et al. (2020), except for small differences (e.g., the rela-

tionships between *‘Crocodylus’ megarhinus* and the clade formed by *Kambara implexidens*, *Trilophosuchus rackhami*, and *Australosuchus clarkae*), whose interpretation is out of the scope of this article. The main and most interesting differences are found in the clade of true crocodiles (*Crocodylus*; Node 44). In our analysis we confirm the close relationship between *C. anthropophagus* and *C. thorbjarnarsoni* (Node 51), already recognized by Brochu & Storrs (2012) on the basis of four synapomorphies (anterodorsal orientation of the external nares, upturned squamosals, quadratojugals that extend to the poster-

odorsal corner of the infratemporal fenestra, and prominent prefrontal knobs). In our case, the relationship between the clade formed by these two species and the rest of true crocodiles is resolved. A basal position within *Crocodylus* of *C. anthropophagus* and *C. thorbjarnarsoni*, already retrieved by Delfino et al. (2020), is noteworthy because it may recall the traditional view of *Crocodylus* as an “out-of-Africa” taxon (Brochu 2000, 2007; Delfino et al. 2007), in contrast with the hypothesis of an Indo-Pacific origin of the genus based on biogeographic models (Nicolai & Matzke 2019) and molecular analysis (Oaks 2011). The latter hypothesis is supported also by the maximum parsimony analysis by Scheyer et al. (2013), according to which *C. palaeindicus* (see below) is regarded as basal to all other *Crocodylus*, although their analysis did not include fossil African *Crocodylus*. More fossils, especially from the Mio-Pliocene, are needed to solve this issue.

The clade formed by *C. anthropophagus* and *C. thorbjarnarsoni* (i.e., Palaeoafrikan *Crocodylus sensu* Cossette et al. 2020) is sister taxon of the crown clade (Node 43), which is rooted on a polytomy between (i) *C. niloticus*, (ii) the clade formed by *C. chechchii* and Neotropical crocodiles, (iii) *C. palaeindicus*, and (iv) the clade of other Indo-Pacific crocodiles. The unresolved relationship between *C. niloticus* (Node 3) and the clade of Neotropical *Crocodylus* (Node 48) prevents verifying the hypothesis that the Nile crocodile is basal to the New World species as suggested in previous works (Brochu 2000; White & Densmore 2001; McAilley et al. 2006; Megathan et al. 2010, 2011; Meredith et al. 2011; Oaks 2011; Pan et al. 2020). In fact, the latter clade also includes *C. chechchii* in our tree, thus supporting the reconstruction by Delfino et al. (2020) that the extant American crocodiles (*C. moreletii*, *C. intermedius*, *C. acutus*, and *C. rhombifer*) are closely related to –and possibly derived from– this Miocene African species. The third clade (Node 16) includes only the late Miocene-Pleistocene *C. palaeindicus*, whose relationships with other Indo-Pacific species remain unresolved. The latter species are grouped into a fourth clade (Node 46), in which *C. palustris* represents the most basal taxon, followed by the clade including *C. siamensis* and the closely-related Pleistocene species *Crocodylus ossifragus* from the Pleistocene of Java, and finally by the clade including *C. mindorensis*, *C. johnstoni*, *C. porosus*, and the pair *C. raninus*-*C. novaeguineae*.

CONCLUSIONS

Thanks to the discovery of Black Sun (THOR16_100BS) in Olduvai DK-E site, we have been able to better frame our knowledge on the cranial anatomy of *C. anthropophagus*, which was hitherto known only on the basis of abundant but fragmentary material (Brochu et al. 2010). Despite taphonomic deformation, the completeness of Black Sun allows confirmation or improved observation of most of the diagnostic characters of *C. anthropophagus* (i.e., morphology and development of the squamosal “horns” and of the crests along the maxillary-nasal sutures). Moreover, thanks to the relatively good preservation of the skull table, its shape and relationships with the rest of the skull can be characterised for the first time.

Our comparative analysis has confirmed the morphological differences between the extinct *C. anthropophagus* and *C. thorbjarnarsoni* from the Plio-Pleistocene of Kenya, and the extant *C. niloticus* (Brochu et al. 2010; Brochu & Storrs 2012). The Kenyan species shows an unambiguous combination of characters associated with markedly larger size compared to the other species (Brochu & Storrs 2012). On the other hand, the differences between *C. anthropophagus* and *C. niloticus* are more subtle. Based on the 1:7 ratio between dorsal cranial length and total body length (Whitaker & Whitaker 2008 and references therein), Black Sun could have been as long as 3.5 m, which is in agreement with the average body lengths recorded for extant *C. niloticus* (Cott 1961). We confirm that the cranial morphology of *C. anthropophagus* is outside the range of variation for *C. niloticus* and *C. suchus*, which lies almost exclusively in biometric variations within its geographic range (Fuchs et al. 1974; Brochu et al. 2010; Nestler 2012). These results are supported by our phylogenetic analysis (Fig. 8), which corroborates the close relationship between Palaeoafrikan *Crocodylus* species, that is, *C. anthropophagus* and *C. thorbjarnarsoni*. The combination of characters observed in these two sister taxa places them at the base of *Crocodylus*, providing a further element to the debate on the African or extra-African origin (e.g., see molecular data by Oaks 2011) of this specious genus.

Crocodylus anthropophagus is so far reported in Africa only at Olduvai Gorge (Fig. 9). However, distinguishing fragmentary remains of this species

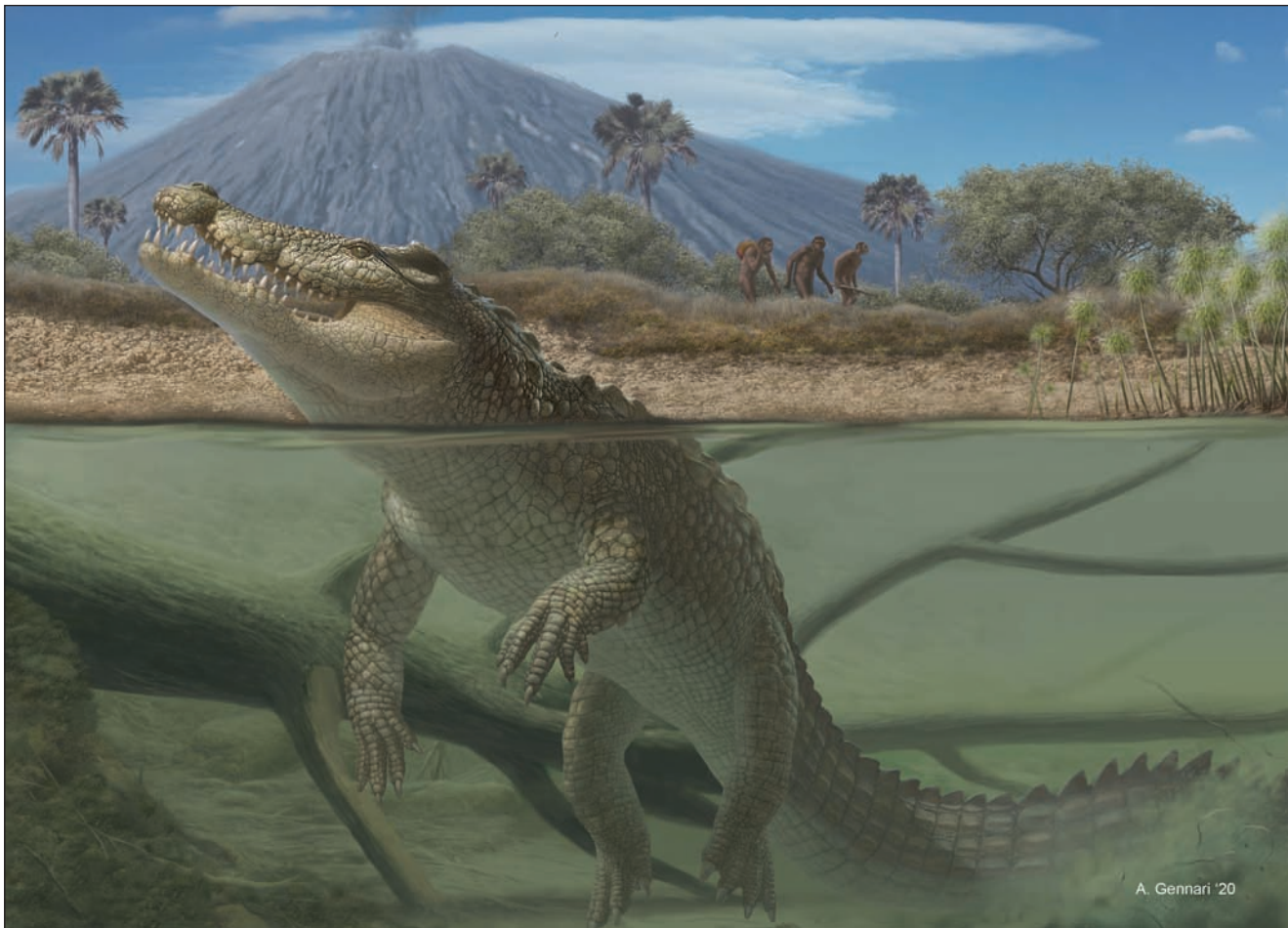


Fig. 9 - Life appearance of *Crocodylus anthropophagus* from Olduvai Gorge (Tanzania) based on the cranial morphology of Black Sun (THOR16_100BS) and information from the literature (Brochu et al. 2010). In the background, some *Homo habilis* individuals are walking in the DK palaeoenvironment about 1.9–1.85 Ma. Artwork by A. Gennari.

from those of *C. thorbjarnarsoni* or *C. niloticus* may not always be possible. Therefore, we are still unable to reconstruct (if any) a broader geographic range of *C. anthropophagus* at least until well-preserved remains are discovered in other African areas. As far as chronology is concerned, Brochu et al. (2010) reported fossils of *C. anthropophagus* from several Olduvai sites/layers, spanning from Bed I to (possibly) Bed IV, i.e., this species occurred for at least the entire Calabrian stage of the Early Pleistocene. Among the previously reported findings, the stratigraphically oldest ones are few postcranial bones (scapula and humerus) from DK (Brochu et al. 2010). Therefore, Black Sun represents to date the earliest (ca. 1.9–1.85 Ma) and, despite not being complete, the most informative cranium of *C. anthropophagus*.

The abundance of crocodile remains in the DK deposits (Masao et al. 2013 and our own dis-

coveries; Fig. 4) suggests that the DK wetland (Fig. 9) was a habitat regularly frequented by these large predators, as well as other areas of the Olduvai Basin (Brochu et al. 2010; Njau & Blumenschine 2012). Taphonomic evidence shows that Olduvai crocodiles fed (at least occasionally) upon hominins (hence the species name *anthropophagus* chosen by Brochu et al. 2010), as crocodile bite marks were detected on at least two hominin specimens, i.e., the left foot OH8 from FLK-NN 3 and the left leg OH35 from FLK-Zinj 22 (Njau & Blumenschine 2012). The first specimen is referred to *H. habilis* (Leakey et al. 1964), the second –whose modifications are not interpreted as crocodile bite marks by some authors (Aramendi et al. 2017)– is tentatively assigned to *H. habilis* (Leakey et al. 1964; Leakey 1971; Day 1978; Susman & Stern 1982; Susman 2008) or *P. boisei* (Day 1976; Tobias 1991). The very abundant crocodile and hominin record (attested by

common stone tools and well-preserved hominin remains such as OH24 and OH56; Leakey 1971; Benito-Calvo & de la Torre 2011; Stanistreet et al. 2018) in DK stimulates more research in this historical site also to clarify the predation risks our early ancestors faced from *C. anthropophagus* (Njau 2012).

Acknowledgments. We sincerely thank all the Italian and Tanzanian participants in the field-workshops of the School of Paleoanthropology of the University of Perugia (<http://www.paleoanthropologia.it>) and of the THOR project (<http://thorproject.it>); their enthusiasm and passion always make research in Tanzania an adventure. Among them, special mention goes to Mirko Lombardi, who coined the name “Black Sun”, and to Filippo Zangrossi, who collaborated in the collection of geological data. The Leakey Camp staff and local Maasai Community are equally acknowledged; our team would not be the same without them. In particular, we thank Agustino Venance, the best fossil hunter in Tanzania, for the discovery of Black Sun, and Daniel Mainoya for the preparation of the specimen. Heartfelt thanks are due to palaeoartist Alberto Gennari for its amazing reconstruction of *C. anthropophagus*. We acknowledge the Tanzania Commission for Science and Technology (COSTECH), the Antiquities Division of the Ministry of Natural Resources and Tourism, and the Ngorongoro Conservation Area Authority (NCAA) for research permits and all their unvaluable support. This research was supported by the School of Paleoanthropology of the University of Perugia (responsible MC) and by the Italian Ministry of Foreign Affairs and International Cooperation (Italian archaeological, anthropological and ethnological missions abroad program; responsible GM). JSK was supported by a scholarship of the Italian Ministry of Foreign Affairs and International Cooperation (Study in Italy program). Comments by Márton Rabi and an anonymous reviewer improved this work.

REFERENCES

- Albert R.M., Bamford M.K., Stanistreet I., Stollhofen H., Rivera-Rondó, C. & Rodríguez-Cintas A. (2015) - Vegetation landscape at DK locality, Olduvai Gorge, Tanzania. *Palaeogeography, Palaeoclimatology, Palaeoecology*, 426: 34-45.
- Aramendi J., Maté-González M.A., Yravedra J., Ortega M.C., Arriaza M.C., González-Aguilera D., Baquedano E. & Domínguez-Rodrigo M. (2017) - Discerning carnivore agency through the three-dimensional study of tooth pits: Revisiting crocodile feeding behaviour at FLK-Zinj and FLK NN3 (Olduvai Gorge, Tanzania). *Palaeogeography, Palaeoclimatology, Palaeoecology*, 488: 93-102.
- Ashley G.M., Carol B., Domínguez-Rodrigo M., Karis A.M., O'Reilly T.M. & Baluyot R. (2014) - Freshwater limestone in an arid rift basin: a goldilocks effect. *Journal of Sedimentary Research*, 84: 988-1004.
- Ashley G.M., de Wet C.B., Barboni D. & Magill C.R. (2016) - Subtle signatures of seeps: Record of groundwater in a Dryland, DK, Olduvai Gorge, Tanzania. *The Depositional Record*, 2: 4-21.
- Ashley G.M., de Wet C.B., Houser L.M. & Delaney J.S. (2020) - Widespread freshwater carbonate in the Olduvai Basin, a precursor to a major eruption in the East African Rift System. *The Depositional Record*, 6: 331-351.
- Benito-Calvo A. & de la Torre I. (2011) - Analysis of orientation patterns in Olduvai Bed I assemblages using GIS techniques: implications for site formation processes. *Journal of Human Evolution*, 61: 50-60.
- Blumenschine R.J., Stanistreet I.G. & Masao F.T. (2012) - Olduvai Gorge and the Olduvai landscape paleoanthropology project. *Journal of Human Evolution*, 2: 247-250.
- Brochu C.A. (2000) - Phylogenetic relationships and divergence timing of *Crocodylus* based on morphology and the fossil record. *Copeia*, 2000: 657-673.
- Brochu C.A. (2001) - Congruence between physiology, phylogenetics, and the fossil record on crocodylian historical biogeography. In: Grigg G., Seebacher F. & Franklin C.E. (Eds) - *Crocodylian biology and evolution*: 9-28. Surrey Beatty & Sons, Sydney.
- Brochu C.A. (2007) - Morphology, relationships, and biogeographical significance of an extinct horned crocodile (Crocodylia, Crocodylidae) from the Quaternary of Madagascar. *Zoological Journal of the Linnean Society*, 150: 835-863.
- Brochu C.A. (2020) - Pliocene crocodiles from Kanapoi, Turkana Basin, Kenya. *Journal of Human Evolution*, 140: 102410.
- Brochu C.A., Njau J.K., Blumenschine R.J. & Densmore L.D. (2010) - A new horned crocodile from the Plio-Pleistocene hominid sites at Olduvai Gorge, Tanzania. *PLoS One*, 5: e9333.
- Brochu C.A. & Storrs G.W. (2012) - A giant crocodile from the Plio-Pleistocene of Kenya, the phylogenetic relationships of Neogene African crocodylins, and the antiquity of *Crocodylus* in Africa. *Journal of Vertebrate Paleontology*, 32: 587-602.
- Bronzati M., Montefeltro F.C. & Langer M.C. (2015) - Diversification events and the effects of mass extinctions on Crocodyliformes evolutionary history. *Royal Society Open Science*, 2: 140385.
- Catt J.A. (1990) - Paleopedology manual. *Quaternary International*, 6: 1-95.
- Cherin M., Iurino D.A., Jackson K. & Masao F.T. (2016) - New material of hyaenids (Mammalia, Carnivora) from Olduvai Gorge, Tanzania (Early Pleistocene). *Bollettino della Società Paleontologica Italiana*, 55: 1-9.
- Cossette A.P., Adams A.J., Drumheller S.K., Nestler J.H., Benefit B.R., McCrossin M.L., Manthi F.K., Juma R.N. & Brochu C.A. (2020) - A new crocodylid from the middle Miocene of Kenya and the timing of crocodylian faunal change in the late Cenozoic of Africa. *Journal of Paleontology*, 94: 1165-1179.
- Cott H.B. (1961) - Scientific results of an inquiry into the ecology and economic status of the Nile crocodile (*Crocodylus niloticus*) in Uganda and Northern Rhodesia. *The Transactions of the Zoological Society of London*, 29: 211-356.
- Cuvier F. (1807) - Sur les différentes espèces de Crocodiles vivans et sur leurs caractères distinctifs. *Annales du Muséum d'Histoire Naturelle Paris*, 10: 8-66.
- Day M.H. (1976) - Hominid postcranial material from Bed I,

- Olduvai Gorge. In: Isaac G.L. & McCown E.R. (Eds) - Human Origins: Louis Leakey and the East African Evidence: 363-374. W.A. Benjamin, California.
- Day M.H. (1978) - Functional interpretations of the morphology of postcranial remains of early African hominids. In: Jolly C.J. (Eds) - Early hominids of Africa: 311-345. Gerald Duckworth and Co. Ltd., London.
- De Celis A., Narváez I. & Ortega F. (2020) - Spatiotemporal palaeodiversity patterns of modern crocodiles (Crocodyliformes: Eusuchia). *Zoological Journal of the Linnean Society*, 189: 635-656.
- Delfino M., Segid A., Yosief D., Shoshani J., Rook L. & Libsekal Y. (2004) - Fossil reptiles from the Pleistocene *Homo*-bearing locality of Buia (Eritrea, northern Danakil Depression). *Rivista Italiana di Paleontologia e Stratigrafia*, 110: 51-60.
- Delfino M., Boehme M. & Rook L. (2007) - First European evidence for transcontinental dispersal of *Crocodylus* (late Neogene of southern Italy). *Zoological Journal of the Linnean Society*, 149: 293-307.
- Delfino M. & Rook L. (2008) - African crocodylians in the Late Neogene of Europe: a revision of *Crocodylus bambolii* Ristori, 1890. *Journal of Paleontology*, 82: 336-343.
- Delfino M. & Rossi M.A. (2013) - Fossil crocodylid remains from Scontrone (Tortonian, Southern Italy) and the late Neogene Mediterranean biogeography of crocodylians. *Geobios*, 46: 25-31.
- Delfino M., Candilio F., Carnevale G., Coppa A., Medin T., Pavia M., Rook L., Urcioli A. & Villa A. (2018) - The early Pleistocene vertebrate fauna of Mulhuli-Amo (Buia area, Danakil Depression, Eritrea). *Bollettino della Società Paleontologica Italiana*, 57: 27-44.
- Delfino M., Iurino D.A., Mercurio B., Piras P., Rook L. & Sardella R. (2020) - Old African fossils provide new evidence for the origin of the American crocodiles. *Scientific Reports*, 10: 1-11.
- Delfino M., Luján À, Abella J., Alba D., Böhme M., Pérez-Ramos A., Tschopp E., Morales J. & Montoya P. (2021) - Late Miocene remains from Venta del Moro (Iberian Peninsula) provide further insights on the dispersal of crocodiles across the late Miocene Tethys. *Journal of Paleontology*, 95: 184-192.
- Eaton M.J., Martin A., Thorbjarnarson J. & Amato G. (2009) - Species-level diversification of African dwarf crocodiles (genus *Osteolaemus*): A geographic and phylogenetic perspective. *Molecular Phylogenetics and Evolution*, 50: 496-506.
- Flint R.F., Sanders J.E. & Rodgers J. (1960) - Diamictite, a substitute term for symmictite. *Geological Society of America Bulletin*, 71: 1809-1810.
- Fuchs K., Mertens R. & Wermuth H. (1974) - Die Unterarten des Nilkrokodils, *Crocodylus niloticus*. *Salamandra*, 10: 107-114.
- Gmelin J. (1789) - Linnei systema naturae. G.E. Beer, Leipzig, 1057 pp.
- Hay R.L. (1976) - The Geology of Olduvai Gorge. University of California Press, Berkeley-Los Angeles-London, 203 pp.
- Iijima M., Takai M., Nishioka Y., Thaug-Htike, Zin-Maung-Maung-Thein, Egi N., Kusuhasi N., Tsubamoto T., Kono T.R. & Hirayama R. (2021) - Taxonomic overview of Neogene crocodylians in Myanmar. *Journal of Vertebrate Paleontology*, e1879100.
- Goloboff P.A., Farris J.S. & Nixon K.C. (2008) - TNT, a free program for phylogenetic analysis. *Cladistics*, 24: 774-786.
- Hekkala E.R., Amato G., DeSalle R. & Blum M.J. (2010) - Molecular assessment of population differentiation and individual assignment potential of Nile crocodile (*Crocodylus niloticus*) populations. *Conservation Genetics*, 11: 1435-1443.
- Isberg S., Combrink X., Lippai C. & Balaguera-Reina S.A. (2019) - *Crocodylus niloticus*. *The IUCN Red List of Threatened Species*, e-T45433088A3010181.
- Johanson D.C., Taieb M. & Coppens Y. (1982) - Pliocene hominids from the Hadar Formation, Ethiopia (1973-1977): stratigraphic, chronologic, and paleoenvironmental contexts, with notes on hominid morphology and systematics. *American Journal of Physical Anthropology*, 57: 373-402.
- Jorayev G., Wehr K., Benito-Calvo A., Njau J. & de la Torre I. (2016) - Imaging and photogrammetry models of Olduvai Gorge (Tanzania) by Unmanned Aerial Vehicles: A high-resolution digital database for research and conservation of Early Stone Age sites. *Journal of Archaeological Science*, 75: 40-56.
- Kälin J.A. (1955) - Zur Stammesgeschichte der Crocodilia. *Revue Suisse de Zoologie*, 62: 347-356.
- Laurenti J.N. (1768) - Specimen Medicum, Exhibens Synopsis Reptilium Emendatum cum Experimentatis Circa Venena et Antiodota Reptilium Austriacorum. J.T. de Trattner, Vienna, 214 pp.
- Leakey L.S.B. (1959) - A new fossil skull from Olduvai. *Nature*, 184: 491-493.
- Leakey L.S.B., Tobias P.V. & Napier J.R. (1964) - A new species of the genus *Homo* from Olduvai Gorge. *Nature*, 202: 7-9.
- Leakey M.D. (1971) - Olduvai Gorge: Volume 3, excavations in Beds I and II, 1960-1963 (Vol. 3). Cambridge University Press, 306 pp.
- Leakey M.D., Clarke R.J. & Leakey L.S.B. (1971) - New hominid skull from bed I, Olduvai Gorge, Tanzania. *Nature*, 232: 308-312.
- Lydekker R. (1886) - Indian Tertiary and Post-tertiary Vertebrata: Siwalik Crocodilia, Lacertilia & Ophidia. *Palaeontologia Indica*, Series X, 103: 209-240.
- Maccagno A.M. (1947) - Descrizione di una nuova specie di "*Crocodylus*" del giacimento di Sahabi (Sirtica). *Atti della Reale Accademia Nazionale dei Lincei, Memorie della Classe di Scienze Fisiche, Matematiche e Naturali*, 81: 63-96
- Mannion P.D., Benson R.B.J., Carrano M.T., Tennant J.P., Judd J. & Butler R.J. (2015) - Climate constrains the evolutionary history and biodiversity of crocodylians. *Nature Communications*, 6: 1-9.
- Markwick P.J. (1998) - Crocodylian diversity in space and time: the role of climate in paleoecology and its implication for understanding K/T extinctions. *Paleobiology*, 24: 470-497.

- Masao F.T., Anton S. & Njau J.K. (2013) - Results of recent investigations of the Oldowan and associated hominid remains at the DK site, Olduvai Gorge: a conservation exercise. Proceedings of the International Symposium "Africa, cradle of humanity: recent discoveries". *Travaux du C.N.R.P.A.H.*, 18: 147-168.
- Masao F.T., Ichumbaki E.B., Cherin M., Barili A., Boschian G., Iurino D.A., Menconero S., Moggi-Cecchi J. & Manzi G. (2016) - New footprints from Laetoli (Tanzania) provide evidence for marked body size variation in early hominins. *eLife*, 5: e19568.
- McAliley L.R., Willis R.E., Ray D.A., White P.S., Brochu C.A. & Densmore III L.D. (2006) - Are crocodiles really monophyletic? - Evidence for subdivisions from sequence and morphological data. *Molecular Phylogenetics and Evolution*, 39: 16-32.
- McHenry L.J. (2004) - Characterization and Correlation of Altered Plio-Pleistocene Tephra Using a "Multiple Technique" Approach: Case Study at Olduvai Gorge. Ph.D. Dissertation, Rutgers University, 381 pp.
- Meganathan P.R., Dubey B., Batzer M.A., Ray D.A. & Haque I. (2010) - Molecular phylogenetic analyses of genus *Crocodylus* (Eusuchia, Crocodylia, Crocodylidae) and the taxonomic position of *Crocodylus porosus*. *Molecular Phylogenetics and Evolution*, 57: 393-402.
- Meganathan P.R., Dubey B., Batzer M.A., Ray D.A. & Haque I. (2011) - Complete mitochondrial genome sequences of three *Crocodylus* species and their comparison within the Order Crocodylia. *Gene*, 478: 35-41.
- Meredith R.W., Hekkala E.R., Amato G. & Gatesy J. (2011) - A phylogenetic hypothesis for *Crocodylus* (Crocodylia) based on mitochondrial DNA: evidence for a trans-Atlantic voyage from Africa to the New World. *Molecular Phylogenetics and Evolution*, 60: 183-191.
- Mook C.C. (1927) - The skull characters of *Crocodylus megarhinus* Andrews. *American Museum Novitates*, 289: 1-8.
- Mook C.C. & Brown B. (1933) - A skull with jaws of *Crocodylus sivalensis* Lydekker. *American Museum Novitates*, 670: 1-10
- Moreno-Bernal J.W., Head J. & Jaramillo C.A. (2016) - Fossil crocodylians from the High Guajira Peninsula of Colombia: Neogene faunal change in northernmost South America. *Journal of Vertebrate Paleontology*, 36: e1110586.
- Nestler J.H. (2012) - A geometric morphometric analysis of *Crocodylus niloticus*: evidence for a cryptic species complex. M.Sc. Dissertation, University of Iowa, 70 pp.
- Nicolai M.P. & Matzke N.J. (2019) - Trait-based range expansion aided in the global radiation of Crocodylidae. *Global Ecology and Biogeography*, 28: 1244-1258.
- Njau J. (2012) - Crocodile Predation and Hominin Evolution: Landscape Paleoanthropology at Olduvai Gorge. Lambert Academic Publishing, Saarbrücken, 340 pp.
- Njau J.K. & Blumenshine R.J. (2012) - Crocodylian and mammalian carnivore feeding traces on hominid fossils from FLK 22 and FLK NN 3, Plio-Pleistocene, Olduvai Gorge, Tanzania. *Journal of Human Evolution*, 63: 408-417.
- Njau J.K., Toth N., Schick K., Stanistreet I.G., McHenry L.J. & Stollhofen H. (2021) - The Olduvai Gorge Coring Project: Drilling high resolution palaeoclimatic and palaeoenvironmental archives to constrain hominin evolution. *Palaeogeography, Palaeoclimatology, Palaeoecology*, 561: 110059.
- Oaks J.R. (2011) - A time-calibrated species tree of Crocodylia reveals a recent radiation of the true crocodiles. *Evolution*, 65: 3285-3297.
- Pan T., Miao J.S., Zhang H.B., Yan P., Lee P.S., Jiang X.Y., Ouyang J.H., Deng Y.P., Zhang B.W. & Wu X.B. (2020) - Near-complete phylogeny of extant Crocodylia (Reptilia) using mitogenome-based data. *Zoological Journal of the Linnean Society*, 2020: zlaa074.
- Potts R. (1984) - Home bases and early hominids. *American Scientist*, 72: 338-347.
- Reck H. (1914) - Erste Vorläufige Mitteilung über den Fund eines fossilen Menschenskelets aus Zentral-afrika. *Sitzungsberichte der Gesellschaft naturforschender Freunde*, 3: 81-95.
- Reti J.S. (2016) - Quantifying Oldowan stone tool production at Olduvai Gorge, Tanzania. *PLoS One*, 11: e0147352.
- Schrenk F., Bromage T.G., Gorthner A. & Sandrock O. (1995) - Paleoeology of the Malawi Rift: vertebrate and invertebrate faunal contexts of the Chiwondo Beds, northern Malawi. *Journal of Human Evolution*, 28: 59-70.
- Shirley M.H., Vliet K.A., Carr A.N. & Austin J.D. (2014) - Rigorous approaches to species delimitation have significant implications for African crocodylian systematics and conservation. *Proceedings of the Royal Society B*, 281: 20132483.
- Sill W.D. (1968) - The zoogeography of the Crocodylia. *Copeia*, 1968: 76-88.
- Scheyer T.M., Aguilera O.A., Delfino M., Fortier D.C., Carlini A.A., Sánchez R., Carrillo-Briceño J.D., Quiroz L. & Sánchez-Villagra M.R. (2013) - Crocodylian diversity peak and extinction in the late Cenozoic of the northern Neotropics. *Nature communications*, 4: 1-9.
- Shirley M.H., Carr A.N., Nestler J.H., Vliet K.A. & Brochu C.A. (2018) - Systematic revision of the living African slender-snouted crocodiles (*Mecistops* Gray, 1844). *Zootaxa*, 450: 151-193.
- Smolensky N.L. (2015) - Co-occurring cryptic species pose challenges for conservation: a case study of the African dwarf crocodile (*Osteolaemus* spp.) in Cameroon. *Oryx*, 49: 584-590.
- Solórzano A., Núñez-Flores M., Inostroza-Michael O. & Hernández C.E. (2020) - Biotic and abiotic factors driving the diversification dynamics of Crocodylia. *Palaeontology*, 63: 415-429.
- Stanistreet I.G., Stollhofen H., Njau J.K., Farrugia P., Pante M.C., Masao F.T., Albert R.M. & Bamford M.K. (2018) - Lahar inundated, modified, and preserved 1.88 Ma early hominin (OH24 and OH56) Olduvai DK site. *Journal of Human Evolution*, 116: 27-42.
- Stanistreet I.G., Stollhofen H., Deino A.L., McHenry L.J., Toth N.P., Schick K.A. & Njau J.K. (2020a) - New Olduvai Basin stratigraphy and stratigraphic concepts revealed by OGCP cores into the Palaeolake Olduvai depocentre, Tanzania. *Palaeogeography, Palaeoclimatology, Palaeoecology*, 554: 109751.

- Stanistreet I.G., Boyle J.F., Stollhofen H., Deocampo D.M., Deino A., McHenry L.J., Toth N., Schick K. & Njau J.K. (2020b) - Palaeosalinity and palaeoclimatic geochemical proxies (elements Ti, Mg, Al) vary with Milankovitch cyclicity (1.3 to 2.0 Ma), OGCP cores, Palaeolake Olduvai, Tanzania. *Palaeogeography, Palaeoclimatology, Palaeoecology*, 546: 109656.
- Steel R. (1973) - Handbuch der Paläoherpetologie, Volume 16: Crocodylia. Fischer-Verlag, Stuttgart, 116 pp.
- Stollhofen H. & Stanistreet I.G. (2012) - Plio-Pleistocene syn-sedimentary fault compartments underpin lake margin paleoenvironmental mosaic, Olduvai Gorge, Tanzania. *Journal of Human Evolution*, 63: 309-327.
- Storrs G.W. (2003) - Late Miocene-Early Pliocene crocodylian fauna of Lothagam, southwest Turkana Basin, Kenya. In: Leakey M.G. & Harris J.M. (Eds) - Lothagam: The Dawn of Humanity in Eastern Africa: 137-159. Columbia University Press, New York.
- Susman R.L. (2008) - Brief communication: evidence bearing on the status of *Homo habilis* at Olduvai Gorge. *American Journal of Physical Anthropology*, 137: 356-361.
- Susman R.L. & Stern J.T. (1982) - Functional morphology of *Homo habilis*. *Science*, 217: 931-934.
- Tobias P.V. (1991) - The skulls, Endocasts, and Teeth of *Homo habilis*. Olduvai Gorge, Volume IV. Cambridge University Press, Cambridge, 921 pp.
- Trutnau L. & Sommerlad R. (2006) - Crocodylians. Their Natural History & Captive Husbandry. Edition Chimaira, Frankfurt, 646 pp.
- Uetz P., Freed P. & Hošek J. (2020) - The Reptile Database, <http://www.reptile-database.org>, accessed 14.10.2020.
- White P.S. & Densmore L.D. (2001) - DNA sequence alignments and data analysis methods: their effect on the recovery of crocodylian relationships. In: Grigg G., Seebacher F. & Franklin C.E. (Eds) - Crocodylian Biology and Evolution: 29-37. Surrey Beatty and Sons, Sydney.
- Wood B. (2011) - Wiley-Blackwell Encyclopedia of Human Evolution. John Wiley & Sons, 1056 pp.

